electronics

MDPI

Article

Hybrid Ant-Swarm Coverage and Routing Optimization for Wireless Sensor Networks

Nimrah Ahmed [1,2], Miguel Angel Luque Nieto [3] and Zain Anwar Ali [4,*]

[1] Department Ingeniería de Comunicaciones, E.T.S.I. Telecommunication, University of Málaga, 29010 Málaga, Spain; nimrah2021@uma.es or nimrah@ssuet.edu.pk
[2] Department of Electronic Engineering, Sir Syed University of Engineering and Technology, Karachi 75300, Pakistan
[3] Institute of Oceanic Engineering, University of Málaga, 29010 Málaga, Spain; luquen@uma.es
[4] Department of Electronic Engineering, Maynooth International Engineering College, Maynooth University, W23 A3HY Maynooth, Ireland
* Correspondence: zainanwar.ali@mu.ie

Abstract

In Wireless Sensor Networks (WSNs), effective network coverage, energy-aware routing and reliable data delivery are major challenges. This paper addresses an intelligent optimized WSN using a two-phase hybrid network, thereby tackling these challenges. In the first phase, a proposed Improved Particle Swarm Optimization (IPSO) algorithm locates the collector node in the best position to achieve full coverage. In the second phase, the proposed Modified Elitist Ant Colony Optimization (MEACO) is used to determine the optimized multi-hop routing paths in terms of energy and delay. To evaluate the strength of the proposed framework, a patient network scenario is formulated where patients and collectors are placed to check baseline performance. In addition, a priority-based QoS Scheduling mechanism is introduced for data transfer, in which priority patients are monitored with the least end-to-end delay, while maintaining network lifetime. Reliable delivery of physiological information is challenged by packet loss and unstable wireless links. The proposed framework improves reliability through link quality evaluation, bounded retransmissions, and route recovery. The simulation results show that the proposed IPSO-MEACO approach improves network coverage by 13.2%, minimizes energy utilization by 14.7%, and drastically reduces end-to-end delay by 58.2% compared with classical algorithms. The results also affirm that the algorithm is suitable for full coverage with minimum end-to-end delay and energy consumption.

Keywords: bio-inspired algorithm; coverage; health care system; optimization; routing; wireless sensor network

Check for updates

Academic Editor: Dionisis Kandris

Received: 12 September 2026
Revised: 16 October 2026
Accepted: 19 October 2026
Published: 22 October 2026

Copyright: © 2026 by the authors. Licensee MDPI, Basel, Switzerland. This article is an open access article distributed under the terms and conditions of the Creative Commons Attribution (CC BY) license.

1. Introduction

WSNs have changed our lifestyle with numerous applications in the field of agriculture [1], military [2], marine environment monitoring [3], health care-related guidance and many more. The key advantages of WSN are autonomous control and real-time observation, which reduce manpower needs. Furthermore, the reduced cost of sensors has made WSN-based monitoring systems gradually economical and smarter than conventional monitoring techniques [4]. Smart and efficient WSN solutions are today's need to cater to the ever-increasing demand of monitoring healthcare in real time [5]. However, it has often been observed that WSN infrastructure experiences signal overlaps, coverage interruptions and variable data routing. This may hinder the provision of critical patient data. Inefficient

energy utilization and inaccurate communication are observed due to the failure of conventional algorithms to adapt to such network conditions. Therefore, designing a WSN that ensures critical data of every patient is covered, transmitted and received with the least amount of delay and energy cost is the main challenge being faced.

The fusion of WSN with bio-inspired algorithms, computing and artificial intelligence research has fabricated a model of ambient intelligence for the challenges in daily life [6]. Integration of advanced optimization algorithms for synchronized coverage and routing is still a major challenge. In early studies, the focus of WSN was coverage [7,8] or routing [9]. In hospitals, especially Intensive Care Units (ICU), patients rely on continuous monitoring of their vitals as their conditions are critical. Wearable sensors collect important health data in real time and transfer it to medical staff wirelessly. WSN has transformed into a promising approach for supporting the data communications of medical devices that monitor patients in the ICU. However, different constraints specific to different hospitals need to be considered, for example, room size, patients and hindrance in transmission, before designing such hybrid systems. Methods need to be adopted that optimize sensing coverage and multi-hop routing while keeping the constraints in view.

With the aim of overcoming these critical issues, this research introduces a novel strategy that proposes a hybrid algorithm for WSN adapted for an ICU environment [10–12]. The proposed algorithm is based on two steps: (i) Improved Particle Swarm Optimization (IPSO), for the best placement of the collector node, and (ii) Modified Elitist Ant Colony Optimization (MEACO), for optimizing the multi-hop routing of data packets with minimal delay and energy consumption.

IPSO: search for the best positions of collector nodes, identified by adaptive inertia weight and time-varying learning coefficients c_1 and c_2 to search and utilize the solution space. Therefore, collector nodes are ideally distributed to maximize coverage and minimize coverage holes, which is vital in ensuring that all patients are within the sensing range of at least one collector.

MEACO: data are forwarded to the nurse station after the algorithm selects the best multi-hop routes, once the collector positions are fixed (by IPSO). A potential routing path is represented by each ant, and its capabilities are evaluated based on total distance, energy and delay. Enhanced route exploration is updated by local pheromone, and elitist reinforcement improves the best global route in different iterations. The patient data are then transferred through multi-hop communication to the nurse station by optimized collector nodes. Unusual readings and critical data that point to emergencies are identified by nurse nodes through incoming information.

Unlike traditional PSO-ACO methods, the framework models ICU patient monitoring as a coupled collector placement and routing challenge. The formation of collectors generated by IPSO is assessed using network-level routing implementation, which impacts the routing exploration of MEACO, reducing redundancy and enabling fast convergence and enhanced transmission of data. Additionally, the framework combines patient-specific clinical urgency into communication decisions. Vital sign irregularities are transformed into priority information so that delay-sensitive physiological packets receive significant communication priority. The proposed MEACO-IPSO framework contribution lies in combining coverage-oriented collector placement and routing optimization within ICU patient-monitoring design. IPSO works to determine collector locations based on patient coverage and communication distance, while MEACO-based multi-hop routing with clinical-priority QoS and link-aware reliable data delivery improves routing decisions for the resultant network topology. The framework further includes priority-based packet scheduling to differentiate emergencies and normal patient data. The framework links collector placement, patient urgency, link quality, retransmission, and route recovery within a unified communication

process within a similar monitoring scenario. The contributions of separate optimization components are also observed through ablation experiments, while consistency is also examined under dynamic and persistent link-failure situations.

Existing WSN approaches frequently optimize individual network objectives such as coverage, energy efficiency or routing, while fewer approaches jointly consider combined objectives. The challenges in this study are collector placement, multi-hop routing, clinical QoS scheduling and reliable data delivery.

The paper is organized as follows: Section 1 introduces the problem statement with the proposed solution, Section 2 discusses the state-of-the-art work, Section 3 presents the system model, and Section 4 focuses on the mathematical model of the proposed algorithm. Finally, Section 5 presents the simulated results and evaluation, while the conclusions and future research are discussed in Section 6.

2. State of the Art Work

Research surveys have been presented that are based on optimized routing and coverage using optimization techniques. Joshi [13] focuses on swarm intelligence-based routing algorithms to boost energy efficiency and improve network performance; the proposed approach can be used for reliable monitoring. This paper discusses a framework that uses a bio-inspired algorithm to enhance node positioning in WSN by balancing coverage and energy consumption and maintaining scalability [14]. Particle Swarm Optimization (PSO) and Ant Colony Optimization (ACO) [15] have revealed robust capabilities in dealing with multi-objective optimization problems by balancing coverage and energy. These algorithms are suitable for heterogeneous WSNs where nodes have different roles and responsibilities. PSO encounters suitable placements of nodes that cover the maximum sensing region [16], while ACO simulates ant hunting behavior to build robust routes depending on the network [17].

Amer presents the CFL-PSO algorithm, which improves coverage in WSN by adjusting router node location, resulting in optimized network performance [18]. In this research, a PSO variant is introduced by balancing exploration and exploitation using oscillatory inertia weight [19]. In this paper, they used two improved versions of the PSO algorithm to solve sensor positioning problems, improving coverage and achieving a longer network lifespan compared with other comparable algorithms [20].

They focus on ACO for routing in WSN, with the aim of controlling congestion and efficient data transmission, resulting in an increase in throughput and a packet delivery ratio, which are useful for healthcare systems [21]. They proposed a better routing technique for effective inter-group routing in ACO by formulating the distance, energy of the hop sensor, and number of preferred probable relay nodes in heuristic data [22]. In [23], an improved variant of Ant Colony Optimization is used, and with the help of shortest path, it is used to determine routing. Two of the biggest consequences of ACO are becoming stuck in local optima and reduced convergence speed. WSNs face challenges in coverage and connectivity. Sensor nodes may be implemented deterministically or randomly. Full coverage is not always required; many applications only need a specified coverage level while maintaining reliable connectivity. Therefore, a key optimization goal is to achieve the necessary coverage and connectivity with the minimum number of sensor nodes while reducing energy consumption and extending network lifetime [24]. Moreover, applying coverage optimization algorithms to the physical world faces many challenges, including energy consumption, addressing 3D coverage in complex environments, and assisting node mobility for initial network coverage issues [25]. The present coverage and routing approaches show significant limitations. ACO routing converges slowly in dense arrangements [26], while PSO is susceptible to impulsive convergence and weak local optima search [27] and degrades when

emergency data loads increase; Hybrid ACO-PSO somewhat mitigates these problems, yet does not merge priority-aware routing. In reference to these gaps, an integrated MEACO IPSO framework has been established.

The literature illustrated above focuses on reducing energy consumption or boosting network coverage, while some concentrate on routing.

3. System Model

The scenario is fabricated to determine the performance of a hybrid bio-inspired optimization system in a 10 × 10 m ICU network. The simulation represents wearable health sensors by synthetically generating physiological data such as heart rate, systolic blood pressure, and oxygen saturation SpO_2) for each patient node and then using those values to determine the emergency of the patient's data packet. For example, specify each patient's synthetic vital sign as follows:

$$V_i = \left[HR_i,\ SpO_{2,i},\ SBP_i\right]. \tag{1}$$

The values are synthetically created within predefined clinically possible ranges, with some patients produced in normal ranges and others in irregular ranges to generate emergency events. The critical states are defined as follows:

$$C_i = \begin{cases} 1, & HR_i > 120 \text{ or } HR_i < 50 \\ & \text{or } SpO_{2,i} < 92 \\ & \text{or } SBP_i > 160 \text{ or } SBP_i < 90, \\ 0, & \text{otherwise,} \end{cases} \tag{2}$$

A priority flag is also introduced, which specifies a medical emergency during the scheduling and routing phase. The value of the priority flag is 1 for critical data and 0 for normal data. Collector nodes C_1-C_3 are implemented as intermediate points to collect data between patients and the nurse station. Each collector records the node ID and optimized (x, y) coordinates. The proposed framework models the ICU as a bounded indoor WSN with controlled communication range, energy-controlled sensor nodes, dynamic patient conditions, clinical-priority traffic, and reliable packet delivery conditions. Designated room-specific RF losses such as exact partition loss, body-shadowing coefficients, and EMI levels are not calibrated because site-specific ICU measurements were inaccessible. Since the ICU is a sensitive clinical place, managing realistic wireless communication experiments needs prior authorization from hospital management and ethical approval. Future work will emphasize hardware-based justification in a planned healthcare environment, subject to the required institutional consents and safety constraints. Wireless technology suitable for architecture is IEEE 802.15.4 [28] as the low power and short range are appropriate for small wearable sensors. The network handles sensitive physiological data over wireless links; security is an important parameter. Wireless transmission may expose patient packets to eavesdropping or unauthorized data modification. To address these risks, a lightweight authenticated-encryption layer can be integrated into the communication process. Ascon-AEAD128 can be applied to shield patient data before wireless transmission. It provides confidentiality by encrypting the physiological payload and integrity/authenticity through an authentication tag. Ascon is considered appropriate for constrained conditions like medical implants, low-power sensors, and IoT devices. The layout is shown in Figure 1 and the flow chart is shown in Figure 2, which describes the organization of work, when the particles are assigned for coverage, and then the pheromone is initialized for the routing mechanism. Table 1 shows the network parameters, Table 2 shows optimization parameters whereas Table 3 shows communication parameters.

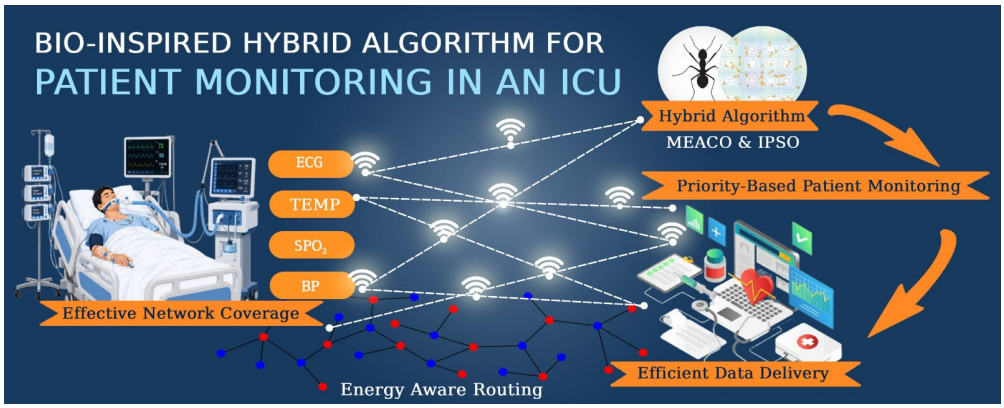


Figure 1. Layout of the setup.

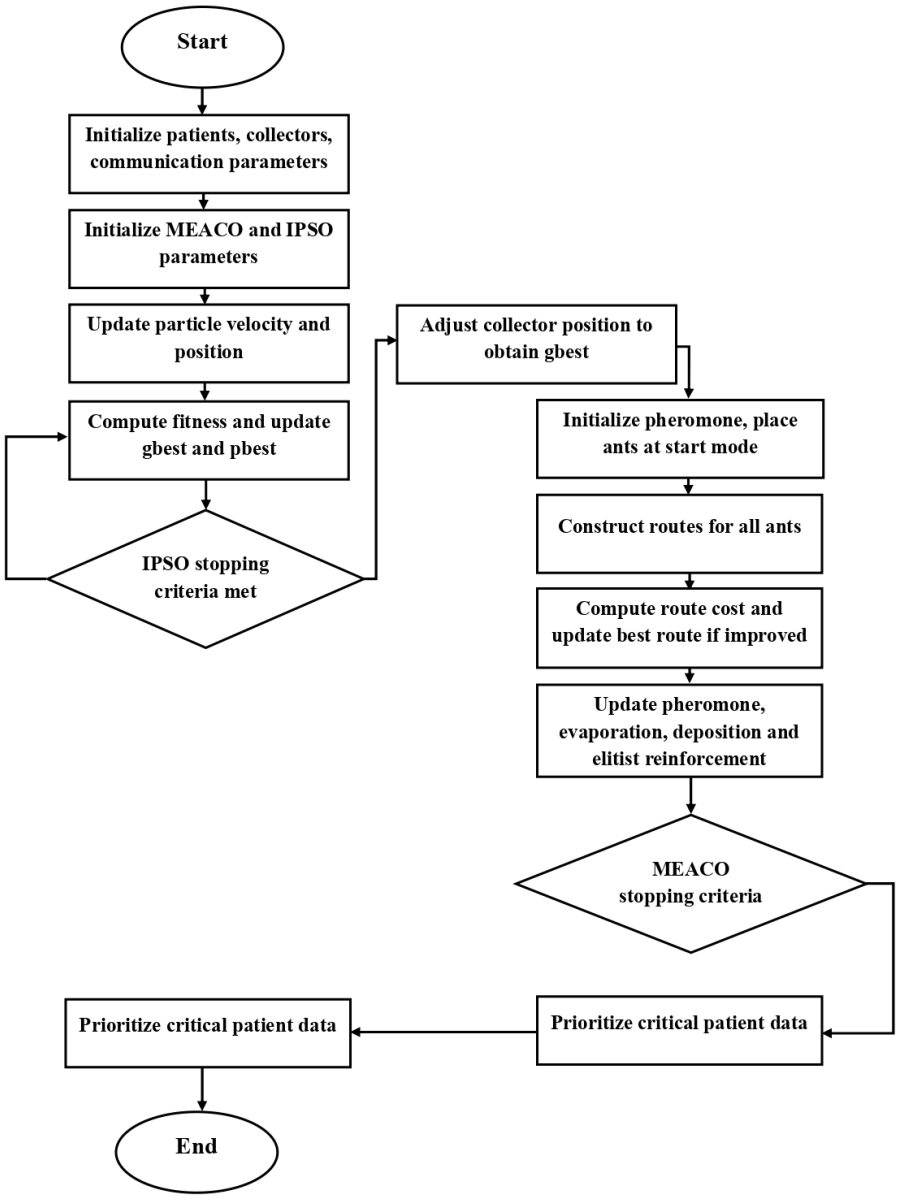


Figure 2. Flowchart of the Proposed Algorithm.

Table 1. Network Parameters.

Parameter	Symbol	Setting
Number of patients	N_P	10 and 20
Number of collectors	N_C	3–7
ICU area	A	10×10 m^2, 15×15 m^2, 20×20 m^2
Sensing range	R_{sr}	3 m
Communication rounds	R	100
Independent runs	N_{run}	10

Table 2. IPSO and MEACO Optimization Parameters.

Parameter	Symbol	Setting
IPSO		
Swarm size	N_s	20
Maximum inertia weight	$\omega_{\max}$	1.1
Minimum inertia weight	$\omega_{\min}$	0.4
Initial cognitive coefficient	$c_{1,\text{initial}}$	2.5
Final cognitive coefficient	$c_{1,\text{final}}$	0.5
Initial social coefficient	$c_{2,\text{initial}}$	0.5
Final social coefficient	$c_{2,\text{final}}$	2.5
Perturbation coefficient	γ	0.03
MEACO		
Number of ants	N_a	20
Evaporation rate	ρ	0.20
Local update coefficient	ξ	0.05
Initial pheromone	τ_0	1.0
Pheromone constant	Q	1.0
Elitist reinforcement coefficient	ϵ	0.05

Table 3. Communication Energy Parameters Used in the ICU WSN Simulation.

Parameter	Symbol	Setting
Packet size	L	400 bits
Transmission electronics energy	$E_{\text{elec,TX}}$	5×10^{-8} J/bit
Reception electronics energy	$E_{\text{elec,RX}}$	5×10^{-8} J/bit
Transmission amplifier coefficient	E_{amp}	1×10^{-9} J/bit/m^2
Path-loss exponent	α	2
Maximum transmission retries	N_{retry}	2

4. Mathematical Model

4.1. Ant Colony Optimization

ACO is inspired by the hunting of food and is a metaheuristic solution where optimization is required [29]. It is based on the best possible way to achieve a solution, using tracks of pheromones left by simulated ants [30]. The pheromones they leave evaporate after some time, and their strength depends on the quality and quantity of edibles available [31]. It is more common for ants to follow tracks with the highest amount of pheromone. ACO algorithm's convergence speed and prediction accuracy are due to its updated pheromone and state transition [32]. Ants produce a good amount of pheromone when hunting, and all ants travel towards the best solution [33]. The probability distribution for selecting the next location is of utmost importance when dealing with a problem [34].

4.2. Modified Elitist Ant Colony Optimization

In this article, Modified Elitist Ant Colony Optimization (MEACO) is presented, which is an improved version presented by Dorigo [35]. What separates the elitist ACO from ACO are elite ants, which can be more than one, and it is their responsibility to update the pheromone trails [36].

4.2.1. Probability

The probability of path finding $P(b,f)$ is determined by the following transfer probability equation from the Elitist Ant System [37].

$$P(b,f) = \begin{cases} \dfrac{(\tau_{bf}(t))^{\alpha}(\eta_{bf})^{\beta}}{\sum_{j\in \mathrm{Av}(b)}(\tau_{bj}(t))^{\alpha}(\eta_{bj}(t))^{\beta}}, & f \in \mathrm{Av}(b), \\ 0, & f \notin \mathrm{Av}(b) \end{cases} \tag{3}$$

where $\tau_{bf}(t)$, $\tau_{bj}(t)$ are the pheromones on the link b to f and b to j respectively, and are controlled by controlling factor α; η_{bf}, η_{bj} are the heuristic on the links b to f and b to j respectively, which is controlled by β; b is the current node, f is the neighboring candidate, and j is the index for all possible neighboring nodes. In this framework, an ant at node b selects its next hop only if it is from a neighboring set $Av(b)$ which contains all nodes that are valid and reachable for ant v during path construction

4.2.2. Heuristic Data

When path finding is in progress, the heuristic can be computed by the combination of distance and delay using weighted normalization [38].

$$\eta = \frac{1}{w_1 d + w_2 D} \tag{4}$$

where d is the Euclidean distance between nodes, which is measured in meters(m), D is the delay in milliseconds (ms), and the weighting ensures that the heuristic remains dimensionless.

4.2.3. Pheromone Update

After the construction of the solution, the pheromone value at a node is updated, and ρ is the evaporation coefficient of pheromone.

$$\tau_{bf}(t+1) = (1-\rho)\tau_{bf}(t) + \rho\Delta\tau_{bf} \tag{5}$$

After the completion of the ant's path, pheromone values are updated, as the hunting ants might leave some additional pheromone.

$$\tau_{bf}(t+1) = (1-\rho)\tau_{bf}(t) + \sum_{v=1}^{m}\Delta\tau_{bf}^{v} \tag{6}$$

where: $\Delta\tau_{bf}^{v}$ is the quantity of pheromone on the node (b, f) left by ant v To accelerate convergence of algorithms, make the pheromone trace more obvious on all the smallest path's edges and route all the elitist ants of the system. Therefore, the above equation for the suitable path formed in every cycle is substituted by the following:

$$\Delta\tau_{bf}^{v} = \frac{Q}{L_v} \tag{7}$$

where Q is a constant pheromone strength and L_v is the total weighted route cost given by the following:

$$L_v = w_d \sum_{i=1}^{n} d_i + w_E \sum_{i=1}^{n} E_i + w_{D_{ETE}} \sum_{i=1}^{n} D_{ETE,i} \tag{8}$$

4.2.4. Local and Global Update

The pheromone is updated by applying local updating rules on the passed node after the pheromone is deposited by the ant.

$$\tau_{bf}(t+1) = (1-\xi)\tau_{bf}(t) + \xi\tau_0 \tag{9}$$

where ξ is the local decay factor and τ_o is the minimum pheromone value. After the arrival of all the ants, the pheromone is updated again by the global updating rule given by the following equation.

$$\tau_{bf}(t+1) = (1-\rho)\tau_{bf}(t) + \rho\Delta\tau_{bf}^{\text{best}} + e\,\Delta\tau_{bf}^{\text{gbest}} \tag{10}$$

where $\Delta\tau_{bf}^{\text{best}}$ contributes to the best path of the iteration, $\Delta\tau_{bf}^{\text{gbest}}$ reinforces the global best routes discovered so far, and e is the Elitist factor, which strongly selects the best ants with lesser delay and energy consumption routes.

4.3. Particle Swarm Optimization

PSO algorithm is systematically based on swarms, in which everyone is known as particles. Every time, particle data are combined to fine-tune each dimensional velocity, which is required for the calculation of the particle's new position. The velocity and distance equations are given by the following equations.

$$v_i(t+1) = \omega v_i(t) + c_1 r_1(p_i - x_i(t)) + c_2 r_2(g - x_i(t)) \tag{11}$$

$$x_i(t+1) = x_i(t) + v_i(t+1) \tag{12}$$

where, v_i is the velocity of particle, $c_1$is the cognitive coefficient, $c_2$is the social coefficient, r_1, r_2 are random numbers in $[0, 1]$, p_i is the personal best position, g is the global best position, ω is the inertia weight, and $x_i(t)$ is the current position of particle.

4.4. Improved Particle Swarm Optimization

In this article, PSO is upgraded to IPSO in terms of ω, c_1 and c_2 [39,40]. Studies believe that the term ω has a significant role in PSO performance. As the changes occur in inertial weight, c_1 and c_2 are also changed over time, such as decreasing over time [41] and can be adjusted by particles developing states [42]. In our proposed algorithm, velocity in Equation (11) is updated as the collector node moves from its existing location towards its global and personal best positions to maximize coverage. Equation (12) shifts the collector node to a new position depending on the updated velocity for better coverage and reduced delay. The parameters are depicted as follows: $x_i(t)$ is the current position of the collector node, p_i is the best location found earlier by the collector node, and g is the best placement among all iterations.

4.4.1. Inertia Weight

In this case, ω is the controlling factor in terms of particle movement, as depicted in the following:

$$\omega = \omega_{\max} - \frac{\omega_{\max} - \omega_{\min}}{\text{maxItr}} \times \text{itr} \tag{13}$$

where *itr* represents the iteration, maxitr is the maximum number of iterations, and ω decreases rapidly from ω_{max} to ω_{min} over the iterations. At the beginning, ω supports broader exploration of the ICU region, letting collector nodes search for different areas for full coverage of patients. Later, ω declines to support complete convergence towards global best positions.

4.4.2. Learning Coefficient

The coefficient c_1 balances the value of the collector's best positions p_i, and c_2 is in charge of balancing the value towards the global best position found by the swarm g. In research, when learning coefficients c_1 and c_2 are set to 2.8 and 1.3, respectively, it was a better version [43]. Initially, c_1 is increasing so collectors can find patients separately. Later, it decreases, as their dependency on personal exploration is lessened by the following equations.

$$c_1(t+1) = c_1(t) - \Delta c_1 \cdot \text{itr} \tag{14}$$

where,

$$\Delta c_1(itr) = \left(\frac{c_{1,\text{start}} - c_{1,\text{end}}}{\text{maxItr}} \right) \times itr$$

Initially, c_2 is small because it is exploring independently. Later it covers all patients, so its value is given by

$$c_2(t+1) = c_2(t) + \Delta c_2 \cdot \text{itr} \tag{15}$$

where in an analogous way,

$$\Delta c_2(itr) = \left(\frac{c_{2,\text{end}} - c_{2,\text{start}}}{\text{maxItr}} \right) \times itr$$

In IPSO iterations, $c_1(itr)$ is gradually decreased from $c_{1,\text{start}}$ to $c_{1,\text{end}}$. During the early exploration stage, collector nodes depend more on their own best locations. As the search proceeds, the self-learning impact is gradually reduced. In contrast, $c_2(itr)$ is gradually increased from $c_{2,\text{start}}$ to $c_{2,\text{end}}$. The increase in c_2 strengthens the influence of the global best location, causing the collector nodes to converge toward the optimal locations within the ICU framework. Finally, the position and velocity of each collector node are updated according to Equations (11) and (12).

4.5. Methodology of Proposed Algorithm

The proposed algorithm starts with the initialization of the ICU setting by describing room boundaries, determining patient sensors as the start point and the nurse station as the end point for routing. At first, the IPSO algorithm is executed to find the best position of collector nodes within the region by updating the positions based on fitness score, coverage and minimal overlap. IPSO continues to improve the collector coordinates till the fitness value is achieved with maximum coverage and minimum redundancy. After the finalization of collector positions, MEACO is applied to make multi-hop routes from the patient to the nurse station. The pheromone and heuristic are updated based on distance and delay on every feasible link. It explores and refines the routes till the most effective route is determined. The path is strengthened by using updated elitist pheromones to speed up the convergence towards the best routing path. A priority-based QoS scheduling method is used to separate emergencies and routine patient traffic. This system is aimed at lowering the queuing delay suffered by emergency patient data before transmission to the nurse station. The IPSO-MEACO model ensures maximum coverage and low-latency routing for monitoring in a WSN-based ICU.

4.5.1. Pseudo Code

The proposed framework combines IPSO for collector-node placement with Modified Elitist Ant Colony Optimization MEACO for optimized data routing. In the beginning, IPSO iteratively adjusts the collector position by revising each particle's velocity and position using the adaptive inertia weight ω, cognitive coefficient c_1, and social coefficient c_2. For each candidate solution, the coverage fitness is evaluated according to the number of patient nodes detected within the sensing range R_{sr}, after which the personal best *pbest* and global

best *gbest* solutions are restructured. This process lasts until the given stopping criterion is fulfilled, and the final *gbest* decides the optimized collector positions. Next, MEACO completes route optimization by utilizing ants from the source node toward the chosen destination. At each hop, sufficient neighboring nodes are found, heuristic information and transition probabilities are determined, and the next hop is probabilistically chosen. A local pheromone update is performed after each selection to maintain exploration, while the entire route is assessed using the defined route-cost function upon reaching the destination. The best route is preserved based on its cost, followed by global pheromone evaporation, route-quality-based pheromone deposition, and elitist reinforcement of the global best route. These procedures are repeated until the MEACO stopping criterion is achieved. Lastly, the optimized routes are used for priority-based QoS scheduling and transmission with reliable data delivery, where clinically critical patient data are given preference over routine traffic to support appropriate delivery of emergency data. The pseudocode is depicted in Algorithm 1.

4.5.2. Priority-Based QoS Scheduling Mechanism

In the proposed framework, Quality of Service (QoS) is executed through static and dynamic clinical priority-based packet scheduling to provide better service to emergency patients. At every round, the patient's physiological parameters, including heart rate (HR), oxygen saturation, and systolic blood pressure, are calculated against defined clinical limits, and the produced packets are categorized as either critical or normal. The packets that are allocated to critical patient situations are given high priority, whereas regular patient information is assigned normal priority. Since the physiological states are also dynamically assessed in scenario 2, a patient's packet priority can change from normal to critical when a sudden abnormal condition occurs and return to normal after recovery. At the scheduling stage, critical packets are placed ahead of normal packets in the transmission queue to reduce the waiting time of emergency data. When two or more packets have the same clinical priority, a First-Come, First-Served (FCFS) policy is used as a tie-breaking mechanism, whereby the packet with the earliest arrival time is served first. Thus, the scheduling order is finalized first by clinical urgency and then by packet arrival time. After scheduling, the packets are transmitted through the optimized MEACO routes toward the collector and then later to the nurse station. Thus, the proposed QoS mechanism distinguishes emergency and routine traffic, and its objective is to lessen the queuing delay of clinically urgent packets while keeping transmission of packets with the same priority.

4.5.3. Reliable Data Delivery Mechanism

Reliable data delivery is a crucial challenge in this framework because physiological data must reach the monitoring station correctly and with minimum packet loss. Wireless links may encounter changes in link quality, interference, limited communication range, and temporary connectivity collapses, which can cause packet transmissions to fail. Multi-hop communication further raises this challenge because failure at any intermediate link can stop a packet from reaching the collector. Furthermore, retransmitting every unsuccessful packet without restriction can increase communication delay and communication energy consumption, which is unwanted for limited-energy sensor nodes. The dilemma becomes more important for emergency patient data, where packet loss or unnecessary delay may decrease the efficiency of timely monitoring. Thus, reliable data delivery needs methods that can identify unsuccessful transmissions, recover from temporary and persistent link failures, and maintain a balance among packet delivery reliability, delay, and communication energy consumption. In the proposed framework, these challenges are addressed through link-quality assessment, bounded retransmissions, and route recovery based on MEACO,

while clinical-priority QoS scheduling supports better service to critical patient packets. The mechanism can be stated in these steps:

Algorithm 1: Hybrid IPSO-MEACO Algorithm for Collector Placement and Routing

Input: Patient locations, collector nodes, communication parameters, and network settings
Output: Optimized collector placement, best routing paths, and improved performance metrics
while *IPSO stopping criterion not fulfilled (coverage convergence or maximum iterations)* **do**
  for *particle* $n = 1, \ldots, k$ **do**
    Revise velocity using ω, c_1, and c_2, and update position according to Equations (9) and (10);
    Compute coverage fitness of patients within sensing range R_{sr} using Equation (15);
    Update personal best (*pbest*) and global best (*gbest*);
  end
end
Adjust collector positions to the obtained *gbest* location;
while *MEACO stopping criterion not fulfilled (route convergence or maximum iterations)* **do**
  for *ant* $v = 1, \ldots, m$ **do**
    Place ant v at the start node;
    while *destination not reached* **do**
      Discover feasible neighboring nodes and compute heuristic values using Equation (2);
      Compute transition probabilities using Equation (1) and select the next node;
      Update local pheromone using Equation (7);
      Move the ant to the selected node and record the route;
    end
    Compute route cost using Equation (6);
    if *current route is better than the existing best route* **then**
      Update best route and route cost;
    end
  end
  Evaporate pheromone on all edges using Equation (3);
  Deposit pheromone according to route quality using Equation (5);
  Apply elitist reinforcement on the global best path using Equation (8);
end
Prioritize QoS scheduling, reliable data delivery and transmission;
return *Optimized collector placement, best routing paths, and improved performance metrics*

1. Choose the next hop: The packet goes to the optimized route decided by MEACO;
2. Test link quality: Before transmission, estimate the chosen link using SNR;

$$SNR_{ij} \geq SNR_{\text{th}} \tag{16}$$

3. If the link quality is not suitable, start MEACO route recovery to choose another feasible next hop;

4. Transmit the packet: If the link quality is acceptable, communicate the patient packet to the chosen next-hop node;
5. Check acknowledgment: The transmitting node waits for an ACK received from the receiver
6. Successful hop: If an acknowledgment is received, the packet is considered positively received at that hop. The process lasts until the next hop is attained;
7. Retransmission: If an acknowledgment is not received, increase the retry counter and retransmit:

$$N_{\text{retry}} = N_{\text{retry}} + 1 \tag{17}$$

8. Check the retry threshold: If

$$N_{\text{retry}} < N_{\max} \tag{18}$$

packet is retransmitted using the link. If

$$N_{\text{retry}} \geq N_{\max} \tag{19}$$

treat the link as persistently inaccurate;
9. MEACO route recovery: Avoid the failed link and find an alternative feasible next hop or route from the point of failure. Transmission then continues the recovered route;
10. Packet loss condition: If no sufficient alternate route exists, attempt retransmission, then record the packet as lost;
11. Updating after delivery: When the packet positively reaches its target, update its PDR, end-to-end delay, communication energy consumption and retransmission count.

4.6. Performance Metrics

4.6.1. Coverage

A patient is considered covered if the distance to at least one collector satisfies the condition $d\left(p_b, c_f\right) \leq R_{sr}$, where $R_{sr} = 3$ m is the sensing range. The distance between patient p_b and collector c_f is calculated using the Euclidean distance, as follows:

$$d(p_b, c_f) = \sqrt{(x_{pb} - x_{cf})^2 + (y_{pb} - y_{cf})^2} \tag{20}$$

An overall coverage ratio is maximized when collector coordinates are updated by IPSO. Coverage fitness is determined by the following:

$$\text{CovFitness} = \frac{N_{\text{covered}}}{N_{\text{Total}}} \tag{21}$$

4.6.2. Packet Delivery Ratio and Throughput

The ratio of packets successfully delivered to the nurse station to the total number of packets sent from every patient sensor is the Packet Delivery Ratio (PDR).

$$\text{PDR} = \frac{NPR_n}{NPS_s} \times 100 \tag{22}$$

where NPR_n is the number of packets received at the nurse station and NPS_s is the number of packets sent by the source node. PDR is a reliability check for an ICU-based WSN. Another usual parameter is the throughput, defined as the reflection of optimized transmission of packets without delay and loss. It can also be stated as the number of packets received per round.

$$\text{Throughput} = \frac{NBR_n}{T_{\text{total}}} \tag{23}$$

where T_{total} represents the total simulation time, and NBR_n represents the number of bits successfully received at the nurse station.

4.6.3. Communication Energy Consumption

A first-order ratio model is used for both transmission E_T and reception E_R in every round for communication energy consumption.

$$E_T = E_{\text{ELEC}} \cdot L + E_{\text{AMP}} \cdot L \cdot d_T^2 \tag{24}$$

$$E_R = E_{\text{ELEC}} \cdot L \tag{25}$$

where E_{ELEC} is the energy consumption by the receiver and transmitter, L is the packet length, E_{AMP} is the dissipated energy, and d_T is the transmission distance. The ICU WSN uses multi-hop clustering, so the total energy consumption E_{Tot} between patients and collectors to nurse stations will be expressed as follows:

$$\begin{aligned} E_{\text{Tot}} = &\sum_{b=1}^{N_p} \left(E_T(d_{p,c}) + E_R(d_{p,c}) \right) \\ &+ \sum_{f=1}^{N_c} \left(E_T(d_{c,n}) + E_R(d_{c,n}) \right) \end{aligned} \tag{26}$$

where, $d_{p,c}$ is the distance of patient to collector, and $d_{c,n}$ is the distance of collector to nurse.

4.6.4. End-to-End Delay

In this case, delay can be computed as follows:

$$D_{\text{ETE}} = D_T + D_{\text{pro}} + D_{\text{Prc}} + D_{\text{que}} \tag{27}$$

where D_T is the transmission delay, $D_{pro}$is the propagation delay, D_{Prc} is the processing delay, and D_{que} is the queue delay.

4.6.5. Fitness Score

In order to balance the proposed algorithm's parameters, multiple performance goals are evaluated by a Fitness parameter.

$$\text{Fitness} = w_{\text{ETE}} \cdot D_{\text{ETE}} + w_E \cdot E \tag{28}$$

where, D_{ETE} is the delay, E is the energy consumption and w_{ETE}, w_E are the weighted functions.

5. Simulations and Discussion

This section discusses the reliability of the proposed method using Matlab Software R2022b version:9.13.

5.1. Scenario 1: Varying Patient Placement

The situation assumes the static locations of patients and active communication patterns between collector nodes. The collector nodes are supposed to have improved computational abilities and serve as collection points to forward data to the nurse station, which serves as a control node and is located at one end of the network. The adjusted layout ensures that every individual patient sensor is within at least one collector node's sensing radius. This makes sure that regions that are overlapping too much or are uncovered are minimized. Thus, an evenly distributed sensing arrangement is provided by the IPSO algorithm. Table 4 shows the synthetic data of medical conditions of patients. The algorithm has been run over 10 independent runs in which 10 patients are scattered in different positions. A round is one communication cycle within the same ICU topology, r = 1, 2 ...10. Simulations are shown for 100 rounds, demonstrating periodic collection of data with respect to time. There

are ten topologies in which IPSO intelligently positions the collector in order to collect data. The simulation generates a new topology only when starting the next independent run.

Table 4. Patient physiological parameters.

Patient ID	Heart Rate (bpm)	SpO_2 (%)	Systolic BP (mmHg)	Condition
1	78	97	120	Normal
2	65	95	110	Normal
3	75	98	119	Normal
4	145	90	150	Critical
5	65	96	105	Normal
6	78	98	125	Normal
7	90	97	120	Normal
8	140	88	185	Critical
9	81	94	120	Normal
10	75	97	116	Normal

Table 5 shows scheduling of Collector C_2 is assigned with four patients: P_1, P_2, P_3 and P_4 in round 100 of run 2 in Figure 3. Patient P_4 experiences critical data with a QoS delay of only 0.0050 s, which makes the total delay 0.0154 s, which is smaller than the delays examined for all normal patients. In contrast, normal patients encounter total delays varying from 0.0204 s to 0.0304 s. This outcome shows the efficiency of the priority-based QoS scheduling method, which provides immediate service to critical patients while continuing transmission for normal patients. Routing delay is the time required for a patient's packet to travel through the wireless network from the patient sensor node toward its allocated collector. It depends on the selected MEACO route and the number of hops. For example, if Patient 4 has a routing delay of 0.0112 s, its packet takes about 11.2 ms to reach Collector C1 through the particular communication route. Queuing delay is the time the packet waits in a queue after entering the collector before it is served or transmitted. In priority-based QoS, critical packets are situated ahead of normal packets, so they should suffer smaller queuing delays.

Table 6, C_3 was assigned with three patients P_6, P_8 and P_9 in round 100 of run 2 in Figure 3. Here, data from patient P_8 are transmitted with less total delay while other patients waited longer. This indicates that collectors prioritized critical information first and dealt with that patient.

Table 5. Patient Scheduling Information for collector C2 in Round 100 of Run2.

Patient	Condition	Priority	Routing Delay (s)	Queuing Delay (s)	Total Delay (s)
1	Normal	0	0.0148	0.0106	0.0254
2	Normal	0	0.0152	0.0152	0.0304
3	Normal	0	0.0124	0.0081	0.0204
4	Critical	1	0.0104	0.0050	0.0154

Table 6. Patient Scheduling Information for collector C3 in Round 100 of Run2.

Patient	Condition	Priority	Routing Delay (s)	Queuing Delay (s)	Total Delay (s)
6	Normal	0	0.0090	0.0216	0.0306
8	Critical	1	0.0156	0.0050	0.0206
9	Normal	0	0.0057	0.0198	0.0256

Table 7, the C_1 collector was assigned with three patients P_6, P_7 and P_8 in round 100 of run 5 in Figure 3. Here, data from patient P_8 are transmitted with less total delay, while

other patients waited longer, whereas in Table 8, the C_3 collector was assigned to three patients, P_1, P_4 and P_9 in round 100 of run 5 in Figure 3. Here, P_4 is transmitted earlier.

Table 7. Patient Scheduling Information for collector C1 in Round 100 of Run5.

Patient	Condition	Priority	Routing Delay (s)	Queuing Delay (s)	Total Delay (s)
6	Normal	0	0.0136	0.0099	0.0235
7	Normal	0	0.0135	0.0050	0.0185
8	Critical	1	0.0061	0.0050	0.0111

Table 8. Patient Scheduling Information for collector C3 in Round 100 of Run5.

Patient	Condition	Priority	Routing Delay (s)	Queuing Delay (s)	Total Delay (s)
1	Normal	0	0.0118	0.0187	0.0305
4	Critical	1	0.0155	0.0050	0.0205
9	Normal	0	0.0074	0.0181	0.0255

Table 9, the C_1 collector was assigned with seven patients P_2, P_4, P_5, P_7, P_8, P_9 and P_{10} in round 100 of run 7 in Figure 3. Here, data from patients P_4 and P_8 are transmitted with less total delay, while other patients waited longer.

Table 9. Patient Scheduling Information for collector C1 in Round 100 of Run7.

Patient	Condition	Priority	Routing Delay (s)	Queuing Delay (s)	Total Delay (s)
2	Normal	0	0.0126	0.0276	0.0402
4	Critical	1	0.0152	0.0051	0.0202
5	Normal	0	0.0077	0.0225	0.0302
7	Normal	0	0.0135	0.0318	0.0452
8	Critical	1	0.0102	0.0050	0.0152
9	Normal	0	0.0100	0.0253	0.0352
10	Normal	0	0.0058	0.0195	0.0252

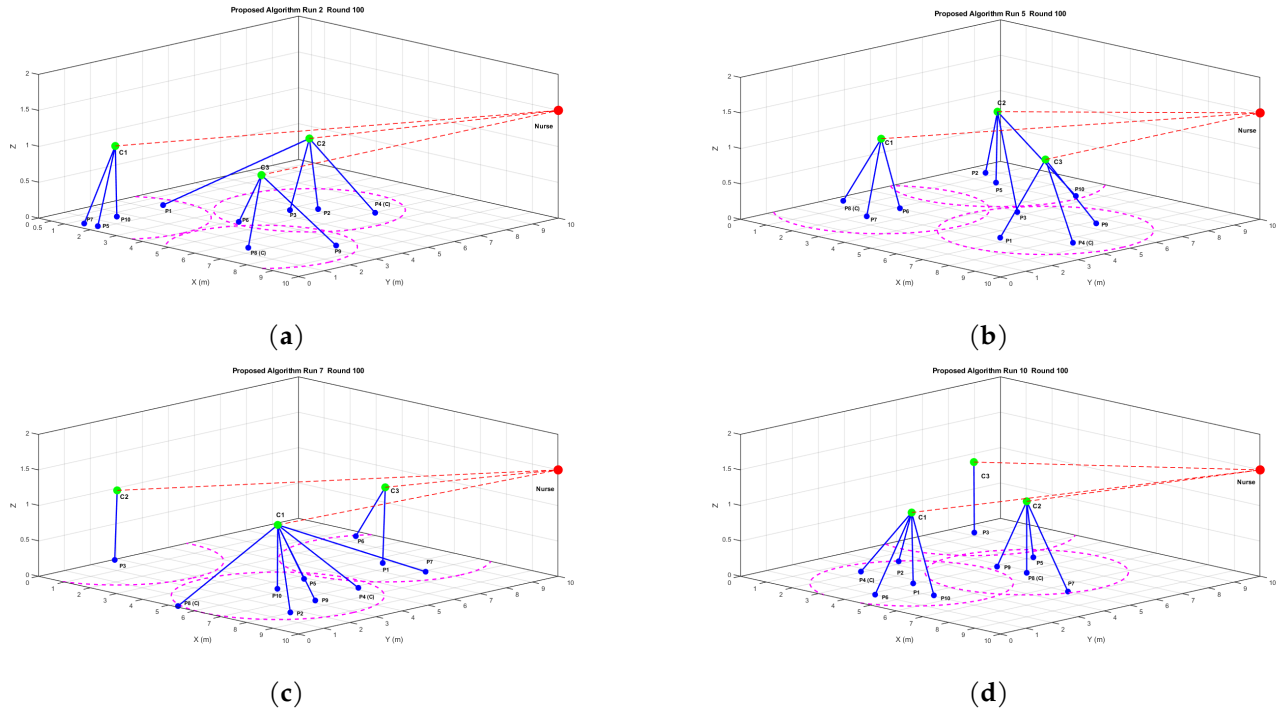
Table 10, the C_1 collector was assigned with five patients P_1, P_2, P_4, P_6, and P_{10} in round 100 of run 10 in Figure 3. Here, data from patients P_4 and P_8 are transmitted with less total delay, while other patients waited longer, whereas in Table 11, the C_2 collector was assigned four patients, P_5, P_6, P_8 and P_9, in round 100 of run 10 in Figure 3. Here, data from patient P_8 are transmitted with minimal delay.

Table 10. Patient Scheduling Information for collector C1 in Round 100 of Run10.

Patient	Condition	Priority	Routing Delay (s)	Queuing Delay (s)	Total Delay (s)
1	Normal	0	0.0142	0.0221	0.0362
2	Normal	0	0.0100	0.0163	0.0262
4	Critical	1	0.0112	0.0050	0.0162
6	Normal	0	0.0110	0.0202	0.0312
10	Normal	0	0.0066	0.0146	0.0212

Table 11. Patient Scheduling Information for collector C2 in Round 100 of Run10.

Patient	Condition	Priority	Routing Delay (s)	Queuing Delay (s)	Total Delay (s)
5	Normal	0	0.0085	0.0147	0.0233
7	Normal	0	0.0091	0.0192	0.0283
8	Critical	1	0.0133	0.0050	0.0183
9	Normal	0	0.0123	0.0210	0.0333



(**a**) (**b**)

(**c**) (**d**)

Figure 3. Patient monitoring under Scenario 1 for 100 round (**a**) Run 2, (**b**) Run 5, (**c**) Run 7, and (**d**) Run 10.

Then calculate the mean and standard deviation stated in Table 12 using the following equations, respectively.

$$\bar{X} = \frac{1}{30}\sum_{r=1}^{30} X_r \tag{29}$$

$$s = \sqrt{\frac{1}{30-1}\sum_{r=1}^{30}\left(X_r - \bar{X}\right)^2} \tag{30}$$

Table 12. Performance comparison of the proposed algorithm with baseline schemes in terms of mean and standard deviation.

Scheme	Coverage (%)	PDR (%)	Energy (J)	Delay (s)	Throughput (bps)	Fitness
MEACO–IPSO	91.51 ± 8.61	90.10 ± 10.56	0.000041 ± 0.000001	0.021982 ± 0.002103	108,359.86 ± 19,115.06	0.011012 ± 0.001052
ACO–PSO	50.82 ± 16.85	33.24 ± 21.27	0.000061 ± 0.000018	0.055922 ± 0.026365	19,266.10 ± 17,447.05	0.027991 ± 0.013190
ACO	56.00 ± 19.56	12.91 ± 18.78	0.000045 ± 0.000003	0.045228 ± 0.005320	8702.13 ± 13,266.05	0.022636 ± 0.002661
PSO	44.90 ± 15.37	23.37 ± 19.96	0.000052 ± 0.000018	0.041431 ± 0.013770	17,112.67 ± 15,932.51	0.020742 ± 0.006893

5.2. Scenario 2: Dynamic Monitoring Under Simultaneous Critical Patient Events

The physiological conditions of every patient, including heart rate, SpO_2 and systolic blood pressure, are updated in each monitoring round. Patients are dynamically categorized as normal or critical corresponding to predefined physiological limits. Thus, a patient's clinical condition may change between consecutive rounds because of simulated emergencies and recovery incidents. While the patient and collector positions remain stationary, the communication settings, patient priorities, routing performance, and packet-delivery performance can change from one round to another. The preferred MEACO routes support both direct and multi-hop transmission. When a patient is close to its assigned collector, its packet is transmitted immediately. Otherwise, nearby patient sensor nodes can act as relay nodes, permitting the packet to reach the collector through multiple hops. For every hop, the framework calculates transmission and reception energy as well. Network coverage

is evaluated according to whether a patient lies within the effective sensing range of at least one collector. The effective sensing range is also influenced by the simulated signal-to-noise ratio, thereby introducing link-quality variation into different communication rounds. When packets reach their corresponding collectors, a priority-based QoS scheduling mechanism manages their transmission towards the nurse station. Critical-patient packets are given higher priority than normal-patient packets. Within the same priority class, packets are served according to their arrival times. Therefore, emergency physiological data are sent before routine monitoring traffic whenever packets go for transmission through the same collector. The total end-to-end delay comprises the routing delay needed to reach the collector and the queuing delay incurred during collector-to-nurse transmission.

Tables 13 and 14 reflecting the round 1 in which patients P_8 and P_4 are critical which are observed by C_1 and C_2, respectively. In round 2, 3 and 4 no critical patient has been observed.

Table 13. Patient Scheduling Information for collector C1 in Round 1.

Patient	Condition	Priority	Routing Delay (s)	Queuing Delay (s)	Total Delay (s)
8	Critical	1	0.0143	0.0050	0.0193
3	Normal	0	0.0084	0.0159	0.0243
10	Normal	0	0.0111	0.0182	0.0293
9	Normal	0	0.0134	0.0208	0.0343
5	Normal	0	0.0136	0.0256	0.0393
1	Normal	0	0.0140	0.0303	0.0443

Table 14. Patient Scheduling Information for collector C2 in Round 1.

Patient	Condition	Priority	Routing Delay (s)	Queuing Delay (s)	Total Delay (s)
4	Critical	1	0.0129	0.0050	0.0179
6	Normal	0	0.0060	0.0169	0.0229
7	Normal	0	0.0142	0.0138	0.0279

Later, in rounds 5, 6 and 7, patient P_5 is critical, which is observed by C_1 as shown in Tables 15–17.

Table 15. Patient Scheduling Information for collector C1 in Round 5.

Patient	Condition	Priority	Routing Delay (s)	Queuing Delay (s)	Total Delay (s)
5	Critical	1	0.0104	0.0050	0.0154
1	Normal	0	0.0108	0.0096	0.0204
10	Normal	0	0.0119	0.0135	0.0254
9	Normal	0	0.0121	0.0183	0.0304
3	Normal	0	0.0124	0.0230	0.0354

Table 16. Patient Scheduling Information for collector C1 in Round 6.

Patient	Condition	Priority	Routing Delay (s)	Queuing Delay (s)	Total Delay (s)
5	Critical	1	0.0132	0.0050	0.0182
9	Normal	0	0.0077	0.0155	0.0232
6	Normal	0	0.0085	0.0197	0.0282
7	Normal	0	0.0098	0.0233	0.0332
3	Normal	0	0.0110	0.0272	0.0382
10	Normal	0	0.0118	0.0313	0.0432

Table 17. Patient Scheduling Information for collector C1 in Round 7.

Patient	Condition	Priority	Routing Delay (s)	Queuing Delay (s)	Total Delay (s)
5	Critical	1	0.0128	0.0050	0.0178
9	Normal	0	0.0059	0.0169	0.0228
3	Normal	0	0.0073	0.0205	0.0278
10	Normal	0	0.0073	0.0255	0.0328
1	Normal	0	0.0129	0.0249	0.0378
7	Normal	0	0.0134	0.0294	0.0428
8	Normal	0	0.0137	0.0341	0.0478

In round 8, patient P_1 is critical and observed by C_3; then, in round 9, the same patient is observed by C_3, which can be seen in Tables 18 and 19.

In round 10, patient P_4 is critical and observed by C_2 in Table 20.

Table 18. Patient Scheduling Information for collector C3 in Round 8.

Patient	Condition	Priority	Routing Delay (s)	Queuing Delay (s)	Total Delay (s)
1	Critical	1	0.0082	0.0050	0.0132
2	Normal	0	0.0086	0.0097	0.0182

Table 19. Patient Scheduling Information for collector C1 in Round 9.

Patient	Condition	Priority	Routing Delay (s)	Queuing Delay (s)	Total Delay (s)
1	Critical	1	0.0120	0.0050	0.0170
3	Normal	0	0.0085	0.0136	0.0220
5	Normal	0	0.0104	0.0166	0.0270
9	Normal	0	0.0115	0.0205	0.0320
10	Normal	0	0.0118	0.0252	0.0370

Table 20. Patient Scheduling Information for collector C2 in Round 10.

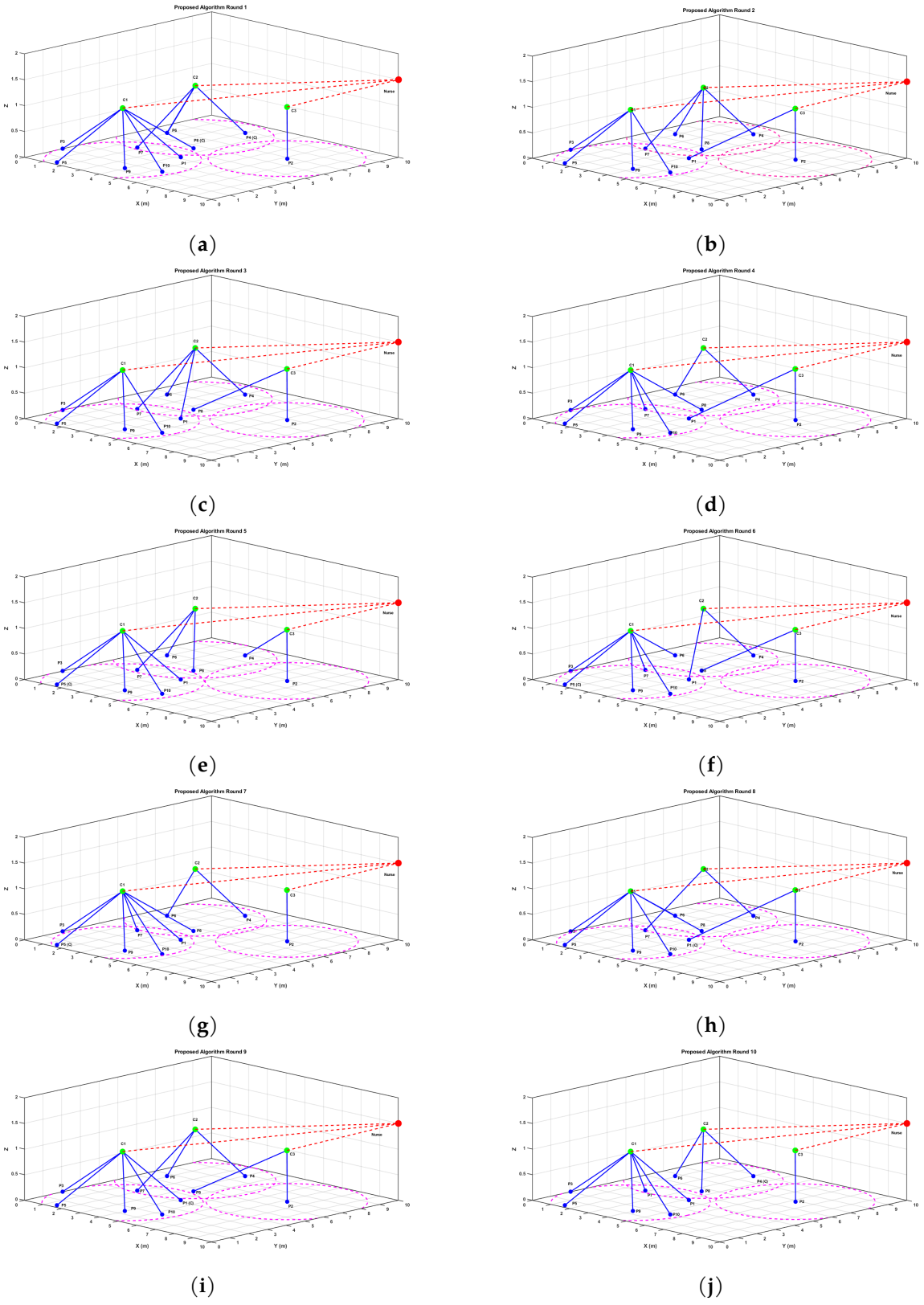
Patient	Condition	Priority	Routing Delay (s)	Queuing Delay (s)	Total Delay (s)
4	Critical	1	0.0139	0.0050	0.0189
6	Normal	0	0.0105	0.0134	0.0239
8	Normal	0	0.0111	0.0178	0.0289

The proposed Algorithm works well when compared with other schemes. A separate network topology is pictured for each round to show patient nodes, critical patients, optimized collectors, sensing ranges, and the connection between collectors and the nurse station, which is illustrated in Figure 4 for 10 rounds. Thus, IPSO specifies optimized and stable collector placement, whereas MEACO constantly determines effective communication routes under varying physiological parameters.

5.3. Scenario 3: Effect of Collector Density on Network Performance

To examine the scalability of the proposed framework, five ICU network configurations (S1, S2, S3, S4, S5) were assessed by adjusting the room dimensions, number of patient nodes, and collector density. The initial configuration consists of a 10 × 10 m ICU with 10 patients and three collectors. The network is then extended to 15 × 15 m with 15 patients and four or five collectors, followed by a 20 × 20 m ICU with 20 patients and six or seven collectors. Each scenario is evaluated over 100 communication rounds and 30 independent runs, using a maximum of 30 optimization iterations. The analysis considers network coverage, PDR, communication energy consumption, end-to-end delay, throughput, optimization

convergence speed, and computational overhead. The paired configurations with similar room measurements and patient populations allow the influence of collector density to be checked independently.



(**a**) (**b**)

(**c**) (**d**)

(**e**) (**f**)

(**g**) (**h**)

(**i**) (**j**)

Figure 4. Patient monitoring under Scenario 2 for different independent runs: (**a**) Run 1, (**b**) Run 2, (**c**) Run 3, (**d**) Run 4, (**e**) Run 5, (**f**) Run 6, (**g**) Run 7, (**h**) Run 8, (**i**) Run 9, and (**j**) Run 10.

5.3.1. Scalability Analysis

The scalability performance was evaluated across five ICU configurations with variable network dimensions, patient populations, and collectors. The outcomes validate that the proposed framework consistently attains higher network coverage, PDR, and throughput while reducing communication energy consumption and end-to-end delay compared with the evaluated ACO–PSO, ACO, and PSO. In the 10 × 10 m scenario, the proposed framework obtains 88.02% coverage and 77.40% PDR, with an average delay of 22.07 ms. As the network dimensions expand, coverage and communication consistency generally decrease. However, increasing the number of collectors from four to five in the 15 × 15 m configuration increases coverage from 72.55% to 81.11% and PDR from 63.63% to 71.44%, while reducing energy consumption and delay. Similar progress is observed in the 20 × 20 m configuration when the collector count increases from six to seven. These results indicate that optimized collector deployment can mitigate performance degradation linked with network expansion and enhance communication efficiency in larger ICU monitoring environments.

5.3.2. Convergence Speed Analysis

The convergence attributes of IPSO and MEACO were assessed across 30 independent runs for each ICU configuration. The outcomes indicate that IPSO generally needs more iterations to reach 95% of its observed fitness upgrade as network size expands. In the small configuration, IPSO requires about 14 iterations, whereas the larger configurations require around 23–25 iterations. In contrast, MEACO reaches the corresponding threshold within around 9–16 iterations across the assessed scenarios, representing comparatively faster stabilization in larger systems. This difference mirrors the separate optimization tasks performed by the two algorithms. IPSO searches for suitable collector spots within a multidimensional exploitation space, while MEACO optimizes communication tracks using pheromone-guided exploration. The outcomes suggest that routing optimization becomes stable relatively quickly, whereas collector placement needs more iterations as network complexity rises.

5.3.3. Optimization Fitness Analysis

The iteration-wise fitness investigation studies the optimization activities of IPSO and MEACO over 30 iterations across the five ICU configurations. Both algorithms demonstrate reliable reductions in their relevant objective functions, representing progressive progress in collector placement and routing results. IPSO obtains a fitness drop ranging from approximately 65.4% to 78.4%, with better improvements observed in several larger configurations. Similarly, MEACO achieves a fitness drop ranging from 22.1% to 47.8%, indicating instant initial improvement tracked by smaller reductions during later iterations. Increasing the number of collectors within the same ICU dimensions also decreases the final IPSO placement fitness, suggesting better placement solutions with extra collectors. However, IPSO maintains fitness improvements near the final iterations, particularly in larger configurations, indicating that further optimization may be possible. Overall, these findings explain the corresponding optimization performance of IPSO and MEACO, maintaining their combination within the proposed framework for ICU-WSN. Tables 21 and 22 show the scalability and convergence of the proposed algorithm.

Table 21. Scalability Performance of the Proposed MEACO-IPSO Framework.

Scenario	Patients	Collectors	Coverage (%)	PDR (%)	Energy (mJ)	Delay (ms)
S1	10	3	88.02	77.40	0.420	22.07
S2	15	4	72.55	63.63	0.677	23.42
S3	15	5	81.11	71.44	0.665	21.40
S4	20	6	69.84	61.33	1.031	24.18
S5	20	7	76.26	66.94	0.977	22.55

Table 22. Convergence Performance of the Proposed MEACO-IPSO Framework.

Scenario	IPSO Iterations	MEACO Iterations	IPSO Fitness Improvement (%)	MEACO Fitness Improvement (%)
S1	14.07	15.67	65.4	22.1
S2	17.50	10.90	73.0	39.6
S3	20.30	11.77	75.6	40.3
S4	24.90	8.83	72.5	47.8
S5	23.43	12.50	78.4	47.2

5.4. Scenario 4: Priority-Based QoS Performance Under Increasing Emergency Traffic

To estimate priority-based communication in the recommended ICU wireless sensor network, emergency and normal packet transmissions were assessed under variable emergency traffic conditions. Five emergency-load scenarios were considered, ranging from 10% to 90%, to examine the effect of rising critical traffic on network functioning. Here, 10% means 10 emergency packets and 90 normal packets, and so on. Emergency packets denoted physiological measurements above predefined critical thresholds, whereas normal packets were normal patient data. Emergency packets were designated a higher transmission priority to decrease communication latency. The scheduling procedure was assessed using mean end-to-end delay and packet delivery ratio. All algorithms were evaluated under the evaluated traffic conditions. The assessment aimed to verify whether the framework could keep preferential transmission of emergency packets while keeping reliable communication for normal patient monitoring. The priority-based QoS performance was assessed under emergency traffic loads varying from 10% to 90%. The outcomes shown in Table 23 show that the proposed MEACO-IPSO framework consistently attains lower emergency-packet delay and higher packet delivery ratio than ACO, PSO, and hybrid ACO-PSO algorithms. At 10% emergency load, MEACO-IPSO obtains an emergency delay of 0.02761 s, which rises to 0.05286 s at 90% load. Despite this increase, the framework keeps a lower emergency delay than all schemes. At 90% emergency load, MEACO-IPSO lowers emergency delay by approximately 19.3%, 42.0%, and 15.7% compared with ACO-PSO, ACO, and PSO, respectively. Additionally, emergency packets experience 37.1% lower delay than normal packets at the peak emergency load, representing regular preferential management of critical traffic. The framework also retains an emergency PDR of approximately 90%, whereas ACO-PSO, PSO, and ACO obtain approximately 37%, 31%, and 20%, respectively. These outcomes indicate that the proposed framework provides favorable latency and delivery performance for emergency traffic under the assessed conditions.

Table 24 shows the average end-to-end delay of emergency and normal packets under variable emergency traffic loads using the proposed framework. The outcome reveals that emergency packets consistently experience lower delays than normal packets across all estimated scenarios. As the emergency traffic load rises, the delays for both packet categories increase due to increased network congestion. However, emergency packets continue to receive preferential treatment, resulting in lower transmission delays. Though the percentage of emergency delay declines under heavier traffic conditions, the proposed

framework retains its ability to prioritize critical patient data. These results demonstrate the efficiency of priority-based scheduling in assisting the appropriate transmission of emergency data in ICU monitoring applications.

Table 23. Comparison of average end-to-end delay under varying emergency traffic loads.

Emergency Load (%)	MEACO–IPSO Delay (s)	ACO–PSO Delay (s)	ACO Delay (s)	PSO Delay (s)
10	0.02761	0.05006	0.07226	0.04770
30	0.03356	0.05330	0.07520	0.05122
50	0.03996	0.05766	0.08093	0.05497
70	0.04640	0.06129	0.08647	0.05900
90	0.05286	0.06551	0.09112	0.06273

Table 24. Comparison of emergency and normal packet delays under varying emergency traffic loads.

Emergency Load (%)	Emergency Delay (s)	Normal Delay (s)	Delay Reduction (%)
10	0.02761	0.05916	53.3
30	0.03356	0.06566	48.9
50	0.03996	0.07201	44.5
70	0.04640	0.07840	40.8
90	0.05286	0.08404	37.1

Table 25 presents the PDR of the proposed framework and the baseline algorithms under variable emergency traffic loads. The outcomes show that the proposed algorithm consistently achieves the highest PDR across all considered scenarios, representing superior packet delivery reliability. As the emergency traffic load expands, the proposed framework keeps stable delivery performance with only minimal fluctuations. In contrast, ACO-PSO, ACO, and PSO present lower PDR values throughout the assessment. These results suggest that the combined collector-placement and routing optimization strategies of MEACO-IPSO keep reliable data transmission under increasing emergency traffic. The consistently high PDR focuses on the framework's capability for maintaining reliable communication for delay-sensitive ICU patient monitoring purposes.

Table 25. Comparison of packet delivery ratio (PDR) under varying emergency traffic loads.

Emergency Load (%)	MEACO IPSO (%)	ACO PSO (%)	ACO (%)	PSO (%)
10	89.99	36.71	20.52	30.23
30	91.10	37.30	20.30	30.62
50	90.31	37.07	20.38	30.64
70	90.53	36.95	20.22	31.15
90	90.53	37.42	20.44	30.83

5.5. Scenario 5: Dynamic Link Failure and Recovery Evaluation

This testing proves how the proposed framework acts when communication links become temporarily inaccessible because of patient movement, body blockage, medical equipment interference, or wireless channel weakening. To estimate communication consistency under dynamic network situations, further simulations were conducted by introducing temporary wireless link failures into the ICU monitoring environment. Different link failure probabilities were considered from 0% to 40%, considering six levels: 0%, 5%, 10%, 20%, 30%, and 40% to denote intermittent channel degradation and communication disruptions. Three configurations were assessed: no recovery, alternate-route recovery, and recovery

combined with packet retransmission. Three failure periods of 1, 3, and 5 communication rounds were investigated to represent temporary, intermediate, and prolonged link interruptions, respectively. A one-round failure denotes a temporary communication disruption, whereas three- and five-round failures show link inaccessibility persisting for three and five consecutive communication rounds. The study considers packet delivery ratio, end-to-end delay, recovery success rate, and communication energy consumption. Link failures were caused dynamically, while the same network requirements were kept across the assessed configurations. This design enables separate measurement of the influence of retransmission and alternative route selection on communication consistency. Each test was conducted over 100 communication rounds, during which introduced link failures continued for 1, 3, or 5 consecutive rounds according to the selected failure period design.

The outcomes show that increasing link-failure probability and duration adversely affects packet delivery consistency, specifically in the absence of a recovery process. The proposed framework demonstrates better performance when alternative route recovery and retransmission are allowed. At a 30% failure probability, continuous for five succeeding rounds, the PDR rises from 27.00% without recovery to 72.00% with route recovery and further to 82.33% when retransmission is included. However, this enhancement has come with an increase in end-to-end delay from 12.61 ms to 47.64 ms, indicating the extra time needed for route restoration and packet retransmission. Under the most serious condition of 40% link failures continuing for five rounds, the joint procedure keeps a PDR of 64.00%, compared with 24.33% without recovery. These outcomes show that integrating route recovery and retransmission considerably increases communication consistency under dynamic link failures, although long disturbances increase latency and limit recovery efficiency. Overall, the results highlight the trade-off between packet delivery reliability and communication delay in the proposed framework. Table 26 presents the performance of MEACO-IPSO under dynamic link failures.

Table 26. Performance of MEACO–IPSO Under Dynamic Link Failures.

Failure (%)	Duration (Rounds)	Recovery Mode	PDR (%)	Delay (ms)
0	1	No recovery	90.33	12.63
0	1	Recovery only	90.33	12.63
0	1	Recovery + retry	100.00	15.39
10	3	No recovery	64.00	12.65
10	3	Recovery only	87.67	25.67
10	3	Recovery + retry	99.00	29.44
20	3	No recovery	54.00	12.63
20	3	Recovery only	86.67	30.49
20	3	Recovery + retry	96.67	33.64
30	5	No recovery	27.00	12.61
30	5	Recovery only	72.00	43.05
30	5	Recovery + retry	82.33	47.64
40	5	No recovery	24.33	12.64
40	5	Recovery only	57.00	39.81
40	5	Recovery + retry	64.00	44.53

5.5.1. Performance Evaluation

The evaluation of performance metrics in terms of coverage, PDR, communication energy consumption, end-to-end delay, throughput and fitness score is shown in Figures 5–8.

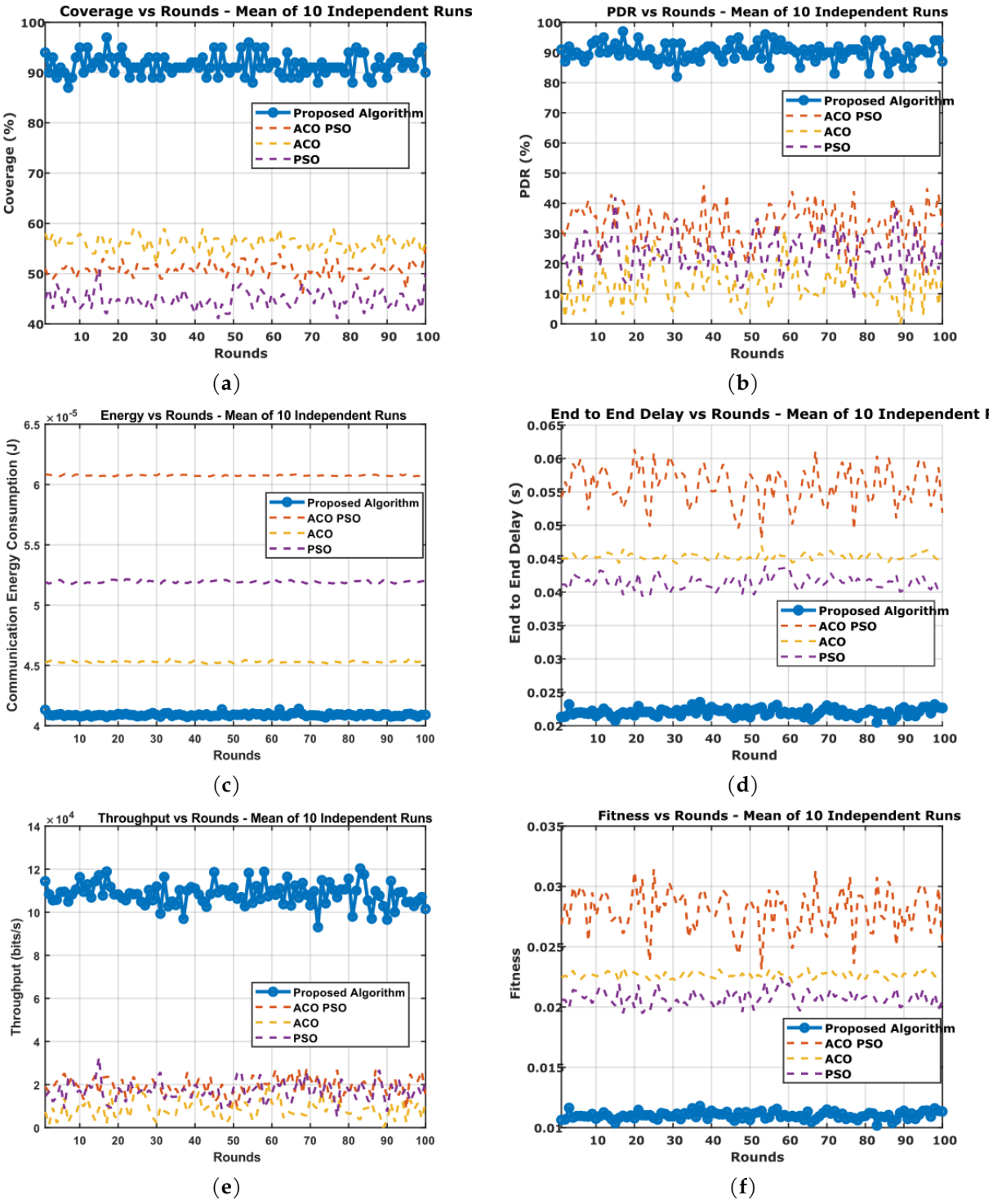


Figure 5. Performance comparison under Scenario 1: (**a**) coverage, (**b**) PDR, (**c**) communication energy consumption, (**d**) end to end delay, (**e**) throughput, and (**f**) fitness.

Coverage

The coverage percentage counts the number of successfully covered patients by any one collector within the pre-defined sensing area. MEACO-IPSO attains higher average coverage by outclassing other schemes, due to the best placement of collectors by IPSO.

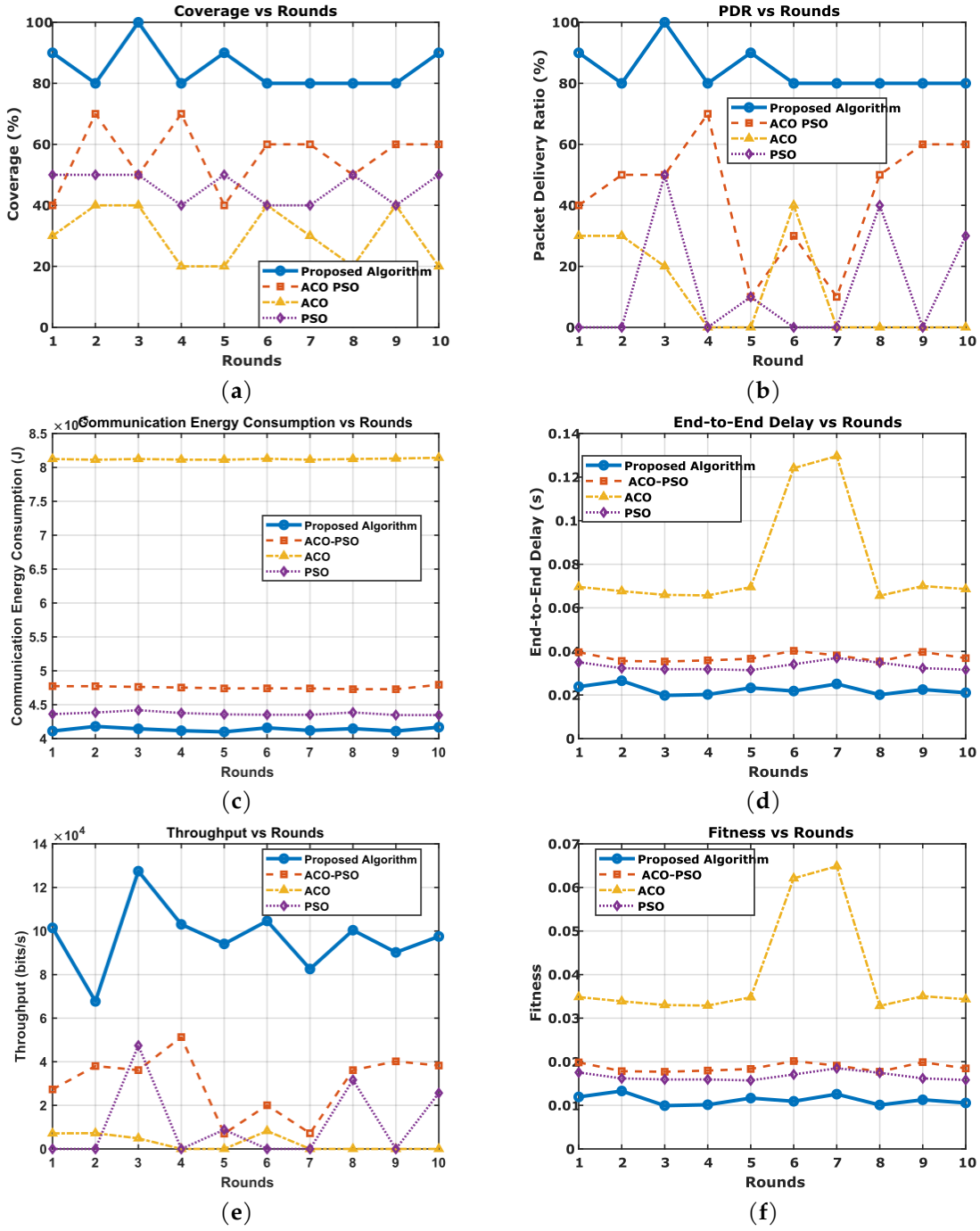


Figure 6. Performance comparison under Scenario 2: (**a**) coverage, (**b**) PDR, (**c**) communication energy consumption, (**d**) end to end delay, (**e**) throughput, and (**f**) fitness.

Packet Delivery Ratio

MEACO-IPSO keeps PDR at its best level due to the mechanism of direct and multi-hop routing. In comparison, ACO-PSO shows reasonable PDR, while other schemes suffer from the selection of inefficient routes and collector positions.

Communication Energy Consumption

MEACO-IPSO maintains a stable and low energy graph due to shorter routing and optimized transmission, while other schemes show an increase due to redundant communication routes.

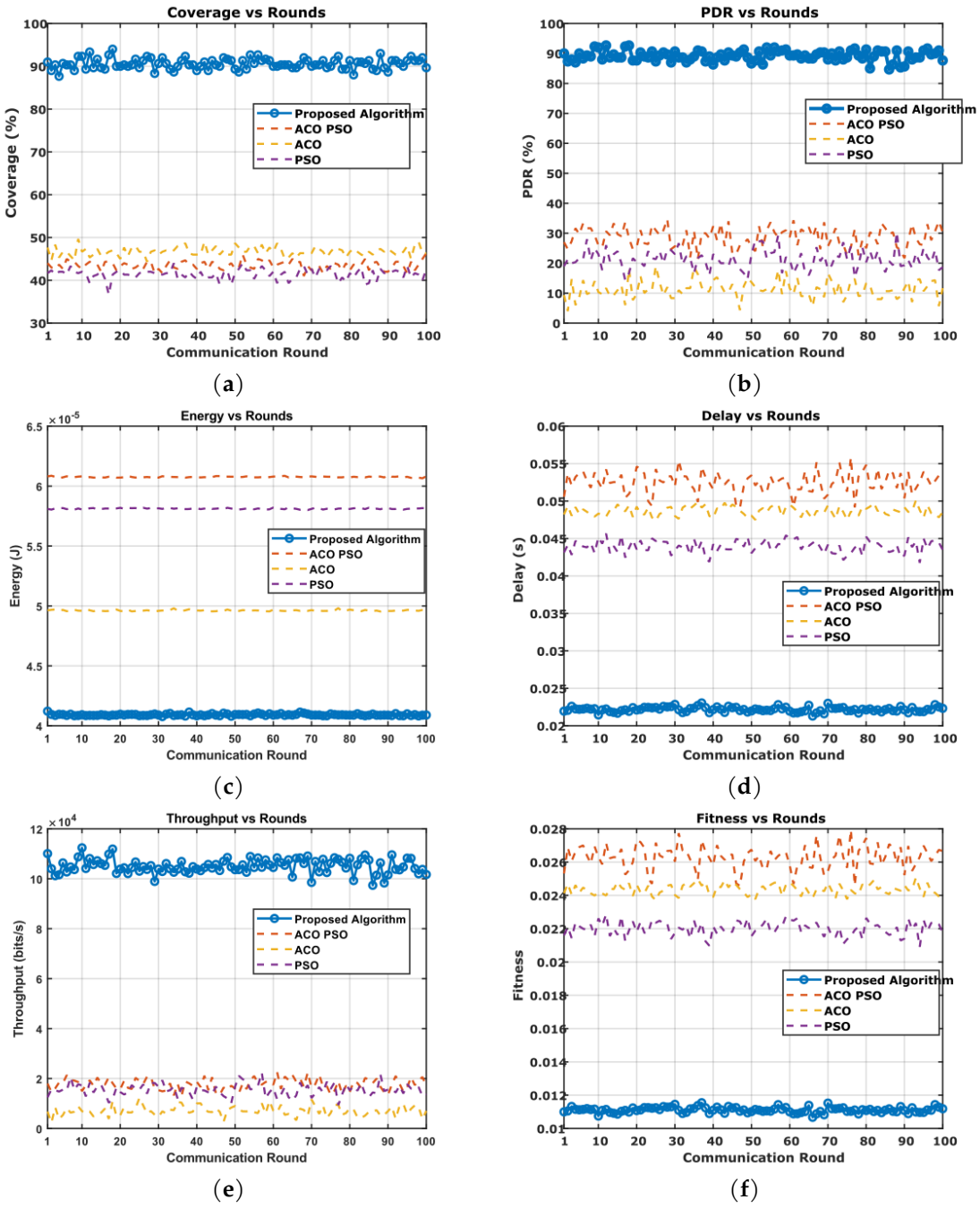


Figure 7. Performance comparison under Scenario 4 (**a**) coverage, (**b**) packet delivery ratio (PDR), (**c**) communication energy consumption, (**d**) end to end delay, (**e**) throughput, and (**f**) fitness.

End-to-End Delay

The proposed algorithm, with the solution of multi-hop routing when required, achieves lower delays compared with other schemes, where delays are high due to prolonged routes towards the nurse station.

Throughput

MEACO-IPSO shows consistently superior throughput performance while ACO-PSO and other schemes lag due to ineffective routing.

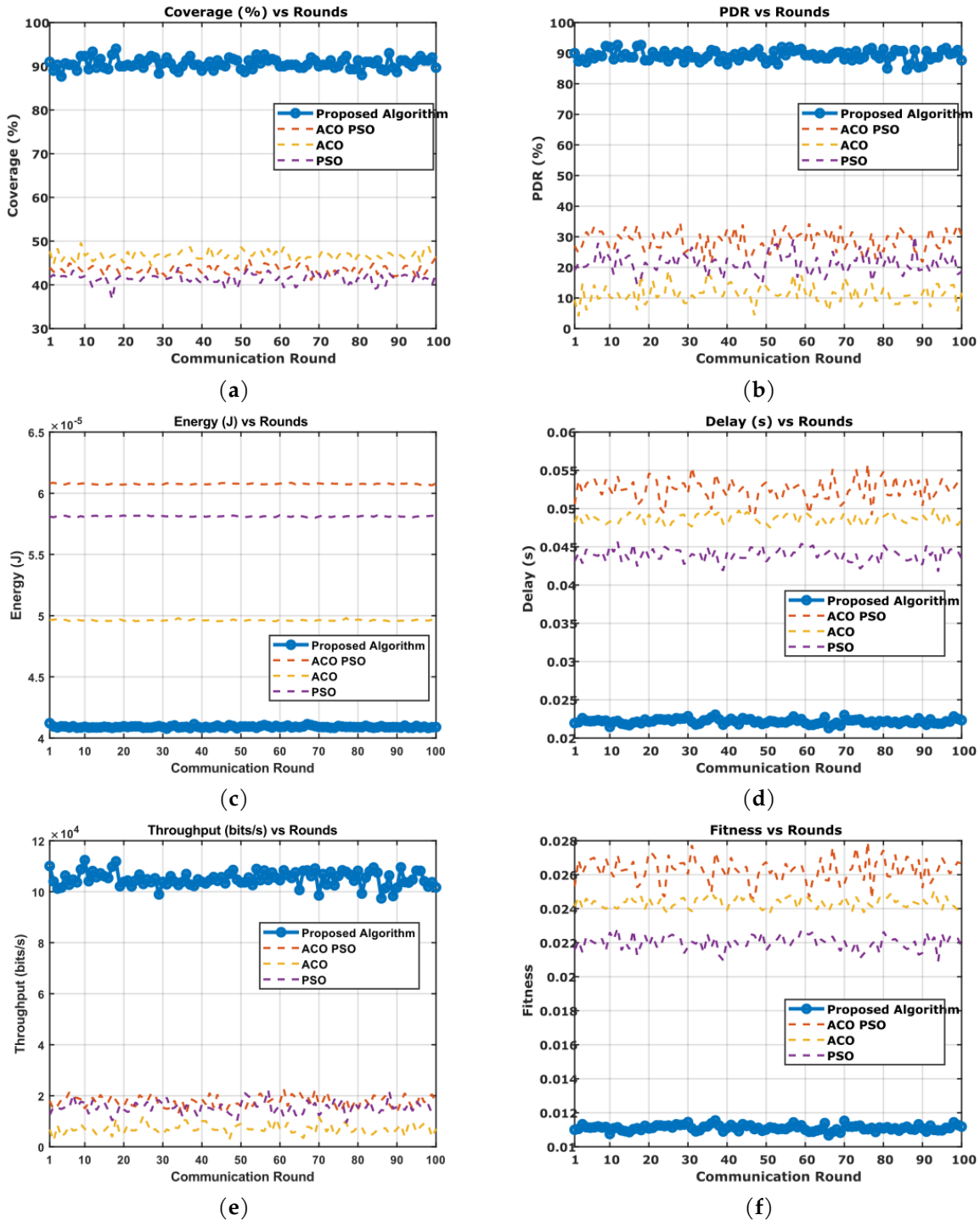


Figure 8. Performance comparison under Scenario 5 (**a**) coverage, (**b**) packet delivery ratio (PDR), (**c**) communication energy consumption, (**d**) end-to-end delay, (**e**) throughput, and (**f**) fitness.

Fitness Score

MEACO-IPSO shows a lower fitness score, which means superior performance, while other schemes produce high costs due to delays and high energy.

Improvements in throughput, end-to-end delay, and energy efficiency arise from IPSO optimization, in which collector placement is based on patient distribution, increasing coverage while minimizing unnecessary patient-to-collector communication distances. This is favorable for communication energy consumption because the transmission energy increases with the communication distance. MEACO subsequently finds efficient multi-hop routes.

By the QoS scheduling mechanism, routing is reduced and queueing overhead contributes to smaller end-to-end delay, while successful delivery of a larger amount of data within a smaller period contributes to better throughput. Thus, the combined collector-placement, routing, priority mechanism and reliability process explains the observed performance advantage over the compared methods.

To examine the individual contributions of the proposed optimization components, an ablation study is conducted using four configurations: IPSO only, MEACO only, PSO-MEACO, and IPSO-ACO. The IPSO-only configuration estimates better collector placement with standard routing, whereas MEACO-only considers modified routing with fixed collector positions. The PSO-MEACO configuration uses conventional PSO to review the contribution of improved collector placement of IPSO. Likewise, IPSO-ACO replaces MEACO with conventional ACO to assess the efficiency of the modified routing method. The complete MEACO-IPSO framework links improved collector placement and modified routing. All four configurations were evaluated in terms of network coverage, packet delivery ratio, end-to-end delay, communication energy consumption, and throughput.

The comparative assessment in Table 27 allows the individual contributions of IPSO and MEACO to be tested and delivers quantitative confirmation of the efficiency of their combination. The study assesses the contributions of collector placement and routing optimization. The results indicate that IPSO only and IPSO ACO achieve the highest mean coverage, PDR, and throughput. MEACO only achieves lower communication energy consumption and end-to-end delay, but its coverage and PDR decline. The PSO MEACO configuration achieves good coverage, indicating an improvement in these metrics when standard PSO is switched to IPSO. Likewise, IPSO ACO lowers delay compared with IPSO only, although its energy consumption rises slightly. These outcomes show that collector placement clearly impacts coverage and packet delivery, while routing optimization influences communication energy consumption and delay. The outcome provides a reasonable evaluation of the impacts of collector placement and routing optimization as shown in Figure 9. The comparison between MEACO IPSO and PSO MEACO separates the effect of changing conventional PSO with IPSO, while the comparison between MEACO IPSO and IPSO ACO inspects the contribution of the modified MEACO routing process. Additionally, IPSO only and MEACO only validate the performance of the individual optimization components. The observed differences in coverage, packet delivery ratio, end-to-end delay, energy consumption, and throughput help in identifying the influence of each component on the overall architecture.

Table 27. Performance Comparison of Ablation Configurations (Mean ± Standard Deviation)

Scheme	Coverage (%)	PDR (%)	Energy (J)	Delay (s)	Throughput (bps)	Fitness
IPSO-only	98.33 ± 3.79	95.47 ± 3.66	$(5.9741 \pm 0.3190) \times 10^{-4}$	0.05543 ± 0.00606	4810.13 ± 187.59	0.46879 ± 0.01181
MEACO-only	72.33 ± 14.31	69.58 ± 13.91	$(4.4889 \pm 0.9250) \times 10^{-4}$	0.04188 ± 0.00576	3504.80 ± 695.57	0.44263 ± 0.02192
PSO + MEACO	97.33 ± 4.50	94.60 ± 4.11	$(5.9815 \pm 0.3500) \times 10^{-4}$	0.04965 ± 0.00393	4766.00 ± 203.70	0.47183 ± 0.01229
IPSO + ACO	98.33 ± 3.79	95.47 ± 3.66	$(6.0353 \pm 0.3420) \times 10^{-4}$	0.05083 ± 0.00446	4810.13 ± 187.59	0.47250 ± 0.01234

5.6. Sensitivity Analysis of Weights

The sensitivity of the optimization weight coefficients was explored using ten parameter configurations. The sensitivity evaluation measured variations in the heuristic weights w_1 and w_2 and the distance, energy, and end-to-end delay weights w_d, w_E, and w_{ETE}, respectively. Table 28 shows the following network coverage, communication delay, and energy consumption, expressed as mean and standard deviation. In Table 28 Heuristic 20/80 is written so that it means 0.2 is w_1 and 0.8 is w_2, as the total sum of weights is 1.

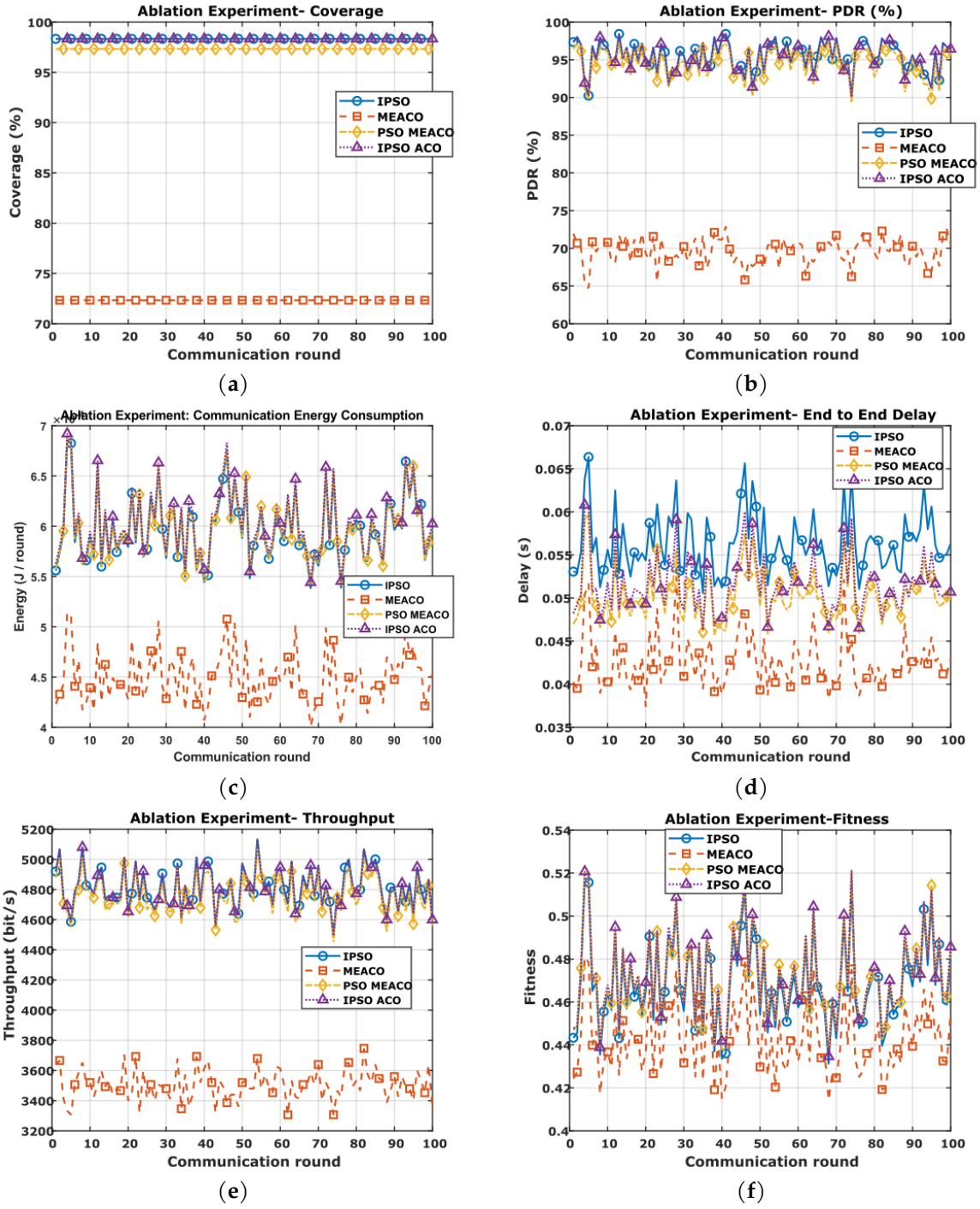


Figure 9. Performance comparison of the ablation configurations: (**a**) coverage, (**b**) packet delivery ratio (PDR), (**c**) communication energy consumption, (**d**) end to end delay, (**e**) throughput, and (**f**) fitness.

The outcomes imply that network coverage stays unchanged across all weight configurations, indicating that the examined parameters mostly influence routing performance rather than collector-placement coverage. However, changes in the optimization weights produce changes in communication delay and energy consumption. The delay-focused configuration obtains the lowest average delay, whereas the distance-focused configuration delivers the least communication energy consumption. Interestingly, giving extreme importance to delay does not further decrease communication latency, demonstrating that optimization performance depends on the interaction among the weighted objectives. Over-

all, the outcomes indicate that proper weight selection can enhance routing efficiency while maintaining reliable network coverage.

Table 28. Parameter Sensitivity Analysis of the Proposed MEACO-IPSO Framework

Configuration	w_1	w_2	w_d	w_E	w_{ETE}	Coverage (%) Mean ± SD	Delay (ms) Mean ± SD	Energy (μJ) Mean ± SD
Reference	0.5	0.5	0.20	0.30	0.50	93.67 ± 5.51	18.523 ± 0.366	41.491 ± 0.182
Heuristic 20/80	0.2	0.8	0.20	0.30	0.50	93.67 ± 5.51	18.424 ± 0.457	41.594 ± 0.204
Heuristic 40/60	0.4	0.6	0.20	0.30	0.50	93.67 ± 5.51	18.458 ± 0.290	41.545 ± 0.136
Heuristic 60/40	0.6	0.4	0.20	0.30	0.50	93.67 ± 5.51	18.483 ± 0.363	41.488 ± 0.186
Heuristic 80/20	0.8	0.2	0.20	0.30	0.50	93.67 ± 5.51	18.483 ± 0.363	41.488 ± 0.186
Distance focused	0.5	0.5	0.50	0.25	0.25	93.67 ± 5.51	18.716 ± 0.042	40.441 ± 0.060
Energy focused	0.5	0.5	0.25	0.50	0.25	93.67 ± 5.51	18.711 ± 0.192	40.530 ± 0.036
Delay focused	0.5	0.5	0.25	0.25	0.50	93.67 ± 5.51	18.396 ± 0.227	41.341 ± 0.130
Balanced fitness	0.5	0.5	0.33	0.33	0.34	93.67 ± 5.51	18.618 ± 0.151	40.638 ± 0.079
Strong delay focus	0.5	0.5	0.10	0.20	0.70	93.67 ± 5.51	18.968 ± 0.301	43.149 ± 0.326

Thus, based on the above simulations, the proposed algorithm showed substantial improvement in all parameters when qualitatively compared with other schemes.

6. Conclusions

The outcome gained maximum network coverage, stable convergence, and produced routes with the least travel area, lowest energy utilization, and reduced delays from one end to another. Positive improvements were observed in the hybrid MEACO-IPSO system over ACO, PSO and hybrid ACO–PSO routing approaches. The model achieved stability and scalability under different conditions by successfully combining the global search strength of IPSO with the MEACO path learning intelligence. Reliable data transfer is ensured between patient wearable sensors and the nurse station, which in turn supports future technological improvements in smart healthcare systems and IoT-based medical systems and networks. The QoS assessment further supported the importance of highlighting emergency patient traffic under variable communication loads. The framework showed comparatively lower transmission delays and higher packet delivery reliability as the percentage of emergency traffic increased. The findings denote that priority-aware scheduling can adjust the sensitivity of critical patient-data transmission while maintaining communication performance for normal monitoring traffic. To assess scalability, the algorithm was assessed across five ICU configurations, with network factors from 10 × 10 m to 20 × 20 m, patient populations varying from 10 to 20 nodes, and collector counts changing from three to seven. The answers showed that enhancing network dimensions presented challenges related to sensing coverage, communication reliability, and energy consumption. However, increasing collector density within the identical network dimensions increased coverage and PDR while reducing communication delay and energy consumption. The convergence assessment further supported improvements in both IPSO placement fitness and MEACO routing fitness over 30 optimization repetitions. IPSO mostly required extra iterations as the deployment space increased, whereas MEACO obtained earlier stabilization in larger configurations. Furthermore, dynamic link-failure tests were supervised to explore the strength of the proposed algorithm under temporary and prolonged communication interferences. Failure possibilities ranging from 0% to 40% and interruption periods of one, three, and five communication rounds were considered. The results proved that alternate-route recovery significantly improved packet delivery consistency. The present work considers this process as a security extension of the suggested framework; complete implementation is left for future experimental investigation.

Author Contributions: N.A.: Methodology, Software, Formal analysis, Writing—original draft, Visualization. M.A.L.N.: Methodology, Software, Writing—review and editing, Visualization. Z.A.A.: Conceptualization, Methodology, Software Validation, Writing—review and editing. All authors have read and agreed to the published version of the manuscript.

Funding: This work was supported by the International Credit Mobility (ICM) Erasmus+ KA-171 program, jointly conducted between Maynooth University, Maynooth, Ireland, and the Sir Syed University of Engineering and Technology, Karachi, Pakistan, under Grant 2025-1-IE02-KA171-HED-000337967.

Data Availability Statement: Synthetic data were used.

Acknowledgments: An artificial intelligence (AI) tool was used during the preparation of this manuscript to assist in developing first figure only. This use of AI did not replace the authors' scientific judgment, critical analysis, or responsibility for the content. The authors have reviewed and verified the manuscript and take full responsibility for its accuracy, originality, and final presentation.

Conflicts of Interest: The authors declared that there are no competing financial interests or personal relationships that could affect the work in this paper.

Abbreviations

The following abbreviations are used in this manuscript:

WSN	Wireless Sensor Networks
ICU	Intensive Care Unit
ACO	Ant Colony optimization
PSO	Particle Swarm optimization
PDR	Packet Delivery Ratio
IPSO	Improved Particle Swarm Optimization
MEACO	Modified Elitist Ant Colony Optimization

References

1. Szewczyk, R.; Osterweil, E.; Polastre, J.; Michael, H.; Mainwaring, A.; Estrin, D. Habitat monitoring with sensor networks. *Assoc. Comput. Mach.* **2004**, *47*, 34–40. [CrossRef]
2. Jain, U.; Hussain, M. Securing Wireless Sensors in Military Applications through Resilient Authentication Mechanism. *Procedia Comput. Sci.* **2020**, *171*, 719–728. [CrossRef]
3. Anwar Ali, Z.; Aamir Khan, M. Development of Wireless Sensor Network Using Long Range Communication for Marine Environment. In *Proceedings of the 17th International Conference on Modelling, Identification and Control*; Springer: Berlin/Heidelberg, Germany, 2026.
4. Muhammad, A.; Ali, Z.A.; Masood, R.J. UAV-Assisted LoRa-Based Wireless Sensor Network for Environmental Monitoring. *Instrumentation* **2025**, *12*, 91–100. [CrossRef]
5. Jovanov, E.; Raskovic, D.; Price, J.; Krishnamurthy, A.; Chapman, J.; Moore, A. A Patient monitoring using personal area networks of wireless intelligent sensors. *Biomed. Sci. Instrum.* **2001**, *37*, 373–378. [PubMed]
6. Cook, D.J.; Augusto, J.C.; Jakkula, V.R. Ambient intelligence: Technologies, applications, and opportunities. *Pervasive Mob. Comput.* **2009**, *5*, 277–298. [CrossRef]
7. Kumar, S.P.; Nagendranath, M.V.S.S.; Alsamri, J. Enhanced Deep Learning-Based Optimization Model for the Coverage Optimization in Wireless Sensor Networks. *Int. J. Comput. Intell. Syst.* **2025**, *18*, 83. [CrossRef]
8. Moslehi, M.M. Exploring coverage and security challenges in wireless sensor networks: A survey. *Comput. Netw.* **2025**, *260*, 96–111. [CrossRef]
9. Pantazis, N.A.; Nikolidakis, S.A.; Vergados, D.D. Energy-Efficient Routing Protocols in Wireless Sensor Networks: A Survey. *IEEE Commun. Surv. Tutor.* **2013**, *15*, 551–591. [CrossRef]
10. Xu, B.; Xu, L.D.; Cai, H.; Xie, C.; Hu, J.; Bu, F. Ubiquitous Data Accessing Method in IoT-Based Information System for Emergency Medical Services. *IEEE Trans. Ind. Inform.* **2014**, *10*, 1578–1586. [CrossRef]
11. Osamy, W.; Khedr, A.M.; Salim, A.; Al Ali, A.I.; El-Sawy, A.A. A review on recent studies utilizing artificial intelligence methods for solving routing challenges in wireless sensor networks. *PeerJ Comput. Sci.* **2022**, *8*, e1089. [CrossRef] [PubMed]
12. Subhashini, P.; Vijayalakshmi, B.A.; VanithaLakshmi, M.; Jeya Ramya, V. Revolutionizing Patient Monitoring in Healthcare with IoT Using WSN and Li-Fi Technology. *J. Opt.* **2024**, *55*, 1203–1211. [CrossRef]

13. Joshi, R.D.; Banu, S. Bioinspired wireless sensor networks—A protocol for an enhanced hybrid energy optimization routing. *Indones. J. Electr. Eng. Comput. Sci.* **2024**, *35*, 1808–1816. [CrossRef]
14. Priyadarshi, R. Efficient node deployment for enhancing coverage and connectivity in Wireless Sensor Networks. *Sci. Rep.* **2025**, *15*, 18132. [CrossRef] [PubMed]
15. Amiri, Z.; Heidari, A.; Zavvar, M.; Navimipour, N.J.; Esmaeilpour, M. The applications of nature-inspired algorithms in internet of Things-based healthcare service: A systematic literature review. *Trans. Emerg. Telecommun. Technol.* **2024**, *35*, e4969. [CrossRef]
16. Nasrollahzadeh, S.; Maadani, M.; Pourmina, M.A. Optimal motion sensor placement in smart homes and intelligent environments using a hybrid WOA-PSO algorithm. *J. Reliab. Intell. Environ.* **2022**, *8*, 345–357. [CrossRef]
17. Priyadarshi, R.; Kumar, R.R. Evolution of swarm intelligence: A systematic review of particle swarm and ant colony optimization approaches in modern research. *Arch. Comput. Methods Eng.* **2025**, *32*, 3609–3650. [CrossRef]
18. Amer, D.A.; Soliman, S.A.; Hassan, A.; Zamel, A.A. Enhancing connectivity and coverage in wireless sensor networks: A hybrid comprehensive learning-Fick's algorithm with particle swarm optimization for router node placement. *Neural Comput. Appl.* **2024**, *36*, 21671–21702. [CrossRef]
19. Han, Y.; Lin, M.; Li, N.; Qi, Q.; Li, J.; Liu, Q. DCWPSO: Particle swarm optimization with dynamic inertia weight updating and enhanced learning strategies. *PeerJ Comput. Sci.* **2024**, *10*, e2253. [CrossRef] [PubMed]
20. Yarinezhad, R.; Hashemi, S.N. A sensor deployment approach for target coverage problems in wireless sensor networks. *J. Ambient. Intell. Humaniz. Comput.* **2023**, *14*, 5941–5956. [CrossRef]
21. Jadhav, S. KFOA: K-mean Clustering, Firefly Based Data Rate Optimization and ACO Routing for Congestion Control in WSN. *Int. J. Electron. Telecommun.* **2023**, *68*, 659–665. [CrossRef]
22. Moussa, N.; El Belrhiti El Alaoui, A. An energy-efficient cluster-based routing protocol using unequal clustering and improved ACO techniques for WSNs. *Peer-to-Peer Netw. Appl.* **2024**, *14*, 1334–1347.
23. Zou, Z.; Qian, Y. Wireless sensor network routing method based on improved ant colony algorithm. *J. Ambient. Intell. Humaniz. Comput.* **2019**, *10*, 991–998. [CrossRef]
24. Sun, Z.; Wu, W.; Wang, H.; Chen, H.; Wei, W. An Optimized Strategy Coverage Control Algorithm for WSN. *Int. J. Distrib. Sens. Netw.* **2014**, *10*, 672487. [CrossRef]
25. Wang, Y.; Li, M. Coverage Control Optimization Algorithm for Wireless Sensor Networks Based on Combinatorial Mathematics. *Math. Probl. Eng.* **2021**, *2021*, 6066379. [CrossRef]
26. Liu, X.; Feng, J.; Zhao, C.; Liu, X. An adaptive routing selection algorithm based on improved ant colony optimization for mobile ad hoc networks. *Int. J. Electron.* **2025**, *113*, 914–936. [CrossRef]
27. Ahmed, G.; Binbeshr, F.; Alzahrani, A.; Othman, M.; Alfarraj, O.; Sheltami, T. Optimal Clustering and Mobile BS Deployment Through Improved PSO. *Arab J. Sci. Eng.* **2025**, *50*, 16243–16262. [CrossRef]
28. *IEEE Std 802.15.4-2024*; IEEE Standard for Low-Rate Wireless Networks. IEEE: New York, NY, USA, 2024.
29. Chatterjee, A.; Kim, E.; Reza, H. Adaptive Dynamic Probabilistic Elitist Ant Colony Optimization in Traveling Salesman Problem. *SN Comput. Sci.* **2020**, *1*, 95. Correction in *SN Comput. Sci.* **2023**, *4*, 751. [CrossRef]
30. Da Silva, A.R. Solving the job shop scheduling problem with ant colony optimization. *arXiv* **2022**, arXiv:2209.05284.
31. Rezvanian, A.; Vahidipour, S.M.; Sadollah, A. An Overview of Ant Colony Optimization Algorithms for Dynamic Optimization Problems. In *Optimization Algorithms*; IntechOpen: London, UK, 2023.
32. Zhu, W.; Cai, W.; Kong, H. Optimal path planning based on ACO in intelligent transportation. *Int. J. Cogn. Comput. Eng.* **2025**, *6*, 441–450. [CrossRef]
33. Czaczkes, T.J.; Heinze, J. Ants adjust their pheromone deposition to a changing environment and their probability of making errors. *Proc. Biol. Sci.* **2015**, *282*, 20150679. [CrossRef] [PubMed]
34. Liu, Y.; Cao, B. A Novel Ant Colony Optimization Algorithm With Levy Flight. *IEEE Access* **2020**, *8*, 67205–67213. [CrossRef]
35. Dorigo, M.; Maniezzo, V.; Colorni, A. Ant system: Optimization by a colony of cooperating agents. *IEEE Trans. Syst. Man Cybern.* **1996**, *26*, 29–41. [CrossRef] [PubMed]
36. Baydogmus, G.K. Solution for TSP/mTSP with improved parallel clustering and elitist ACO. *Comput. Sci. Inf. Syst.* **2023**, *20*, 195–214. [CrossRef]
37. Zhang, Y.; Wang, Y.J.; Li, H.; Chang, J.B.; Yu, J.Q. A Firefly Algorithm and Elite Ant System-Trained Elman Neural Network for MPPT Algorithm of PV Array. *Int. J. Photoenergy* **2022**, *2022*, 5700570. [CrossRef]
38. Zhang, X.; Cui, X.; Zheng, S. Heuristic Task Scheduling Algorithm Based on Rational Ant Colony Optimization. *Chin. J. Electron.* **2014**, *23*, 311–314. [CrossRef]
39. Kessentini, S.; Barchiesi, D. Particle Swarm Optimization with Adaptive Inertia Weight. *Int. J. Mach. Learn. Comput.* **2015**, *5*, 368–373. [CrossRef]
40. Wang, D.; Tan, D.; Liu, L. Particle swarm optimization algorithm: An overview. *Soft Comput.* **2017**, *22*, 387–408. [CrossRef]
41. Ratnaweera, A.; Halgamuge, S.K.; Watson, H.C. Self-organizing hierarchical particle swarm optimizer with time-varying acceleration coefficients. *IEEE Trans. Evol. Comput.* **2004**, *8*, 240–255. [CrossRef]

42. Ide, A.; Yasuda, K. A basic study of adaptive particle swarm optimization. *Electr. Eng. Jpn.* **2005**, *151*, 41–49. [CrossRef]
43. Clerc, M.; Kennedy, J. The particle swarm-explosion, stability and convergence in a multi-dimensional complex space. *IEEE Trans. Evol. Comput.* **2022**, *6*, 58–73.

Disclaimer/Publisher's Note: The statements, opinions and data contained in all publications are solely those of the individual author(s) and contributor(s) and not of MDPI and/or the editor(s). MDPI and/or the editor(s) disclaim responsibility for any injury to people or property resulting from any ideas, methods, instructions or products referred to in the content.